

A quantum algorithm for dynamic mode decomposition integrated with a quantum differential equation solver

Yuta Mizuno^{1,2,3,*} and Tamiki Komatsuzaki^{1,2,3,4}

¹*Research Institute for Electronic Science, Hokkaido University, Sapporo, Hokkaido 001-0020, Japan*

²*Institute for Chemical Reaction Design and Discovery (WPI-ICReDD), Hokkaido University, Sapporo, Hokkaido 001-0021, Japan*

³*Graduate School of Chemical Sciences and Engineering, Hokkaido University, Sapporo, Hokkaido 060-8628, Japan*

⁴*SANKEN, Osaka University, Ibaraki, Osaka 567-0047, Japan*

(Dated: April 23, 2024)

We present a quantum algorithm that analyzes time series data simulated by a quantum differential equation solver. The proposed algorithm is a quantum version of the dynamic mode decomposition algorithm used in diverse fields such as fluid dynamics and epidemiology. Our quantum algorithm can also compute matrix eigenvalues and eigenvectors by analyzing the corresponding linear dynamical system. Our algorithm handles a broad range of matrices, in particular those with complex eigenvalues. The complexity of our quantum algorithm is $O(\text{poly log } N)$ for an N -dimensional system. This is an exponential speedup over known classical algorithms with at least $O(N)$ complexity. Thus, our quantum algorithm is expected to enable high-dimensional dynamical systems analysis and large matrix eigenvalue decomposition, intractable for classical computers.

I. INTRODUCTION

Quantum algorithms provide exponential speedups over classical algorithms for numerical linear algebra tasks such as eigenvalue decomposition of unitary or Hermitian matrices [1–3], singular value decomposition of low-rank matrices [4, 5], and solving linear systems of equations [6, 7]. These quantum algorithms can solve problems of N dimensions in runtime $O(\text{poly log } N)$. They have significant applications in quantum chemistry [8], machine learning [4, 9], and solving differential equations [10–15].

Quantum numerical linear algebra offers prospects for advancements in dynamical systems analysis. A probability density function on the state space of a dynamical system is advanced in time by the Perron–Frobenius operator [16, 17]. Meanwhile, the Koopman operator is responsible for the time evolution of observable functions on the state space [16, 17]. These operators are linear operators on infinite-dimensional function spaces. In other words, any finite-dimensional (possibly nonlinear) dynamical system can be described as an infinite-dimensional linear dynamical system. Therefore, linear algebraic techniques such as spectral decomposition can be applied to general dynamical systems analysis. Such an infinite-dimensional linear operator may be numerically approximated by a finite-dimensional matrix through a suitable truncated basis expansion. Although this finite-dimensional approximation may lead to a linear dynamical system with an extremely-large number of dimensions $N(\gg 1)$, quantum computing has a potential to handle such high-dimensional systems.

A quantum linear differential equation solver (QLDES)

can simulate an N -dimensional linear dynamical system with a sparse coefficient matrix in runtime $O(\text{poly log } N)$ [10–12, 14, 15]. One can also simulate some nonlinear dynamical systems efficiently by a QLDES combined with Carleman linearization [13], which is essentially the same as a truncated basis expansion described above. These quantum solvers yield quantum states whose amplitudes encode simulated time series data. However, the tomography of such quantum states takes a runtime of $O(N)$, so that $O(N)$ time and memory space are required to read out the entire time series data as classical data. Therefore, an efficient method for extracting essential dynamical information from the quantum data is highly demanded to achieve an exponential speedup in dynamical systems analysis [18].

We propose a novel quantum algorithm for dynamic mode decomposition (DMD) integrated with a QLDES, which achieves an exponential speedup in dynamical systems analysis over known classical counterparts. The DMD is a numerical technique that estimates the spectral decomposition of the Koopman operator of a dynamical system from its time series data [16, 19]. This spectral decomposition elucidates essential temporal behavior of the dynamical system. Classical DMD algorithms are frequently applied in various fields such as fluid dynamics and epidemiology [16]. Given that these fields are expected as potential targets of quantum differential equation analysis [13, 18], our quantum DMD (qDMD) algorithm should enhance the dynamical systems analysis in these fields using quantum computers.

Although quantum algorithms for the spectral estimation from time series data have been proposed by Steffens et al. [20] and Xue et al. [21], these algorithms mainly focus on the analysis of time series data provided as classical data. Because constructing such a classical data structure requires $O(N)$ time and memory space, they might be unable to analyze high-dimensional

* mizuno@es.hokudai.ac.jp

data when N is too large for classical computers to handle. In contrast, our qDMD algorithm aims to analyze time series data embedded in quantum states computed by a QLDES. Our framework integrates simulation and data analysis seamlessly on a quantum computer, achieving the overall dynamical systems analysis with $O(\text{poly log } N)$ complexity. A detailed comparison of these algorithms is provided in Supplemental Material.

Our qDMD algorithm also serves as a quantum subroutine for eigenvalue decomposition of matrices, especially those with complex eigenvalues essential in quantum scattering problems [22]. If a linear differential equation $\dot{\mathbf{x}} = \mathbf{A}\mathbf{x}$ can be simulated efficiently on a quantum computer, our algorithm can efficiently compute approximate eigenvalues and eigenvectors of $\exp(\Delta t \mathbf{A})$, where Δt is the time step of the simulation. Notably, the matrix \mathbf{A} is not restricted to Hermitian and may have complex eigenvalues. Therefore, the integrated framework of a QLDES and the qDMD algorithm can be considered as a generalization of quantum phase estimation [1–3], which combines Hamiltonian dynamics simulation and quantum Fourier transform. Although previous studies [22–25] have pioneered quantum eigensolvers for complex eigenvalue problems, these approaches have limitations such as the lack of the theoretical guarantee of an exponential speedup and requiring a specific form of input states (see Supplemental Material for details). Our qDMD algorithm is designed to be free from such limitations.

II. DYNAMIC MODE DECOMPOSITION

We introduce the *exact DMD* algorithm proposed by Tu et al. [19]. Let us consider an N -dimensional linear dynamical system $\dot{\mathbf{x}} = \mathbf{A}\mathbf{x}$, where $\mathbf{x} \in \mathbb{C}^N$, and $\mathbf{A} \in \mathbb{C}^{N \times N}$ is a diagonalizable matrix¹. Let \mathbf{K} denote the time evolution operator with time step Δt : $\mathbf{K} := \exp(\Delta t \mathbf{A})$. Suppose we have a collection of M snapshot pairs of time-series data, symbolized as $\{(\mathbf{x}_j, \mathbf{x}'_j)\}_{j=0}^{M-1}$. Here \mathbf{x}'_j signifies the state observed at the subsequent time step following \mathbf{x}_j : $\mathbf{x}'_j \approx \mathbf{K}\mathbf{x}_j$ ². Note that \mathbf{x}_j 's can be taken from multiple different trajectories. From the data, we can estimate the time-evolution operator \mathbf{K} as

$$\tilde{\mathbf{K}} = \underset{\mathbf{J} \in \mathbb{C}^{N \times N}}{\text{argmin}} \|\mathbf{X}' - \mathbf{J}\mathbf{X}\|_{\text{F}} = \mathbf{X}'\mathbf{X}^+, \quad (1)$$

where $\tilde{\mathbf{K}}$ signifies the approximation of the underlying \mathbf{K} , $\|\cdot\|_{\text{F}}$ denotes the Frobenius norm, $\mathbf{X} := [\mathbf{x}_0 \cdots \mathbf{x}_{M-1}]$, $\mathbf{X}' := [\mathbf{x}'_0 \cdots \mathbf{x}'_{M-1}]$, and \mathbf{X}^+ is the

pseudo-inverse of \mathbf{X} . The construction of $N \times N$ matrix $\tilde{\mathbf{K}}$ and its eigenvalue decomposition becomes intractable as N increases. Thus, we solve the eigenvalue problem of the following projected matrix instead:

$$\tilde{\mathbf{K}}' = \mathbf{Q}^\dagger \tilde{\mathbf{K}} \mathbf{Q}, \quad (2)$$

where \mathbf{Q} is an $N \times R$ matrix whose columns are the R dominant left singular vectors of the $N \times 2M$ matrix $[\mathbf{X} \ \mathbf{X}']$. The effective rank R is determined so that the error of the rank- R approximation of $[\mathbf{X} \ \mathbf{X}']$ in the Frobenius norm is less than a specified tolerance. The exact DMD algorithm typically assumes that R is sufficiently smaller than N so that the eigenvalue decomposition of the $R \times R$ matrix $\tilde{\mathbf{K}}'$ is tractable by a (classical) computer. The eigenvalue decomposition of $\tilde{\mathbf{K}}'$ approximates that of $\tilde{\mathbf{K}}$ as³

$$\tilde{\lambda}_r \approx \tilde{\lambda}'_r, \quad \tilde{\mathbf{w}}_r \approx \mathbf{Q}\tilde{\mathbf{w}}'_r \quad (r = 1, \dots, R). \quad (3)$$

Here, $\tilde{\lambda}_r$ and $\tilde{\mathbf{w}}_r$ (resp. $\tilde{\lambda}'_r$ and $\tilde{\mathbf{w}}'_r$) are the r -th eigenvalue and eigenvector of $\tilde{\mathbf{K}}$ (resp. $\tilde{\mathbf{K}}'$). The real part and the imaginary part of $(\ln \tilde{\lambda}_r)/\Delta t$ correspond to the decay/growth rate and the oscillation frequency of the r -th DMD mode, respectively. The computational complexity of this algorithm is $O(\min(NM^2, MN^2))$ for the singular value decomposition (SVD) and $O(R^3)$ for the eigenvalue decomposition of $\tilde{\mathbf{K}}'$ [26].

III. qDMD ALGORITHM

Our qDMD algorithm consists of the following five steps:

1. Prepare quantum states encoding \mathbf{X} , \mathbf{X}' , and $[\mathbf{X} \ \mathbf{X}']$ using a QLDES.
2. Compute the SVDs of \mathbf{X} , \mathbf{X}' , and $[\mathbf{X} \ \mathbf{X}']$ on a quantum computer.
3. Estimate the elements of $\tilde{\mathbf{K}}'$ from the quantum data and construct $\tilde{\mathbf{K}}'$ as classical data.
4. Solve the eigenvalue problem of $\tilde{\mathbf{K}}'$ on a classical computer.
5. Compute a quantum state encoding $\tilde{\mathbf{w}}_r$.

Steps 1–3, and 5 are efficiently executed on a quantum computer in runtime $O(\text{poly log } N)$ as shown below. Given that $R \ll N$, step 4 can be handled by a classical computer. Consequently, our qDMD algorithm is exponentially faster than its classical counterpart with

¹ For the case that A is not diagonalizable, see discussion in Supplemental Material.

² Since numerical integration of a linear differential equation involves approximations, the simulated data \mathbf{x}'_j is an approximation of the exact solution $\mathbf{K}\mathbf{x}_j$.

³ Without the rank truncation, the eigenvalues and eigenvectors of $\tilde{\mathbf{K}}'$ are exactly those of $\tilde{\mathbf{K}}$ and all of the nonzero eigenvalues of $\tilde{\mathbf{K}}$ are identified by the algorithm [19]. However, the rank truncation generally leads to an approximation error.

respect to N . Similar quantum-classical hybrid strategies are also employed by Steffens et al. [20] and Xue et al. [21], though their methods perform steps 1 and 2 using quantum oracles of classical time series data and the specifics of the quantum procedures differ from our algorithm (see also Supplemental Material for algorithm comparison).

In what follows, we will expound the quantum procedures of steps 1–3 and 5. Henceforth, we adopt the following notation: The computational basis whose bit string represents integer i is denoted by $|i\rangle$. As necessary, we denote a ket vector of the k -th quantum register like $|\cdot\rangle_k$. For vector $\mathbf{v} = (v^0, \dots, v^{n-1})^\top \in \mathbb{C}^n$, we define $|\mathbf{v}\rangle := \sum_{i=0}^{n-1} v^i |i\rangle$ (unnormalized). Similarly, for matrix $\mathbf{Z} = [\mathbf{v}_0 \cdots \mathbf{v}_{m-1}] \in \mathbb{C}^{n \times m}$, we write $|\mathbf{Z}\rangle := \sum_{j=0}^{m-1} |\mathbf{v}_j\rangle |j\rangle = \sum_{i=0}^{n-1} \sum_{j=0}^{m-1} v_j^i |i\rangle |j\rangle$. A normalized matrix $\mathbf{Z}/\|\mathbf{Z}\|_F$ is denoted by $\hat{\mathbf{Z}}$, thus $|\hat{\mathbf{Z}}\rangle$ symbolizes the normalized ket vector (quantum state) proportional to $|\mathbf{Z}\rangle$. Additionally, the r -th singular value, left and right singular vectors of matrix \mathbf{Z} are designated by σ_r^Z , \mathbf{u}_r^Z , and \mathbf{v}_r^Z , respectively. The notation of quantum circuit diagrams we employ can be found in [27].

A. Step 1

First, we prepare a quantum state encoding matrix \mathbf{X} . In this article, we consider preparing time series data of L different trajectories of T time steps, thus the number of columns M equals TL . In addition, we normalize the time scale in units of the simulation time step $\Delta t \leq 1/\|\mathbf{A}\|_2$ ($\|\cdot\|_2$ denotes the spectral norm) for convenience. We assume a quantum oracle U_0 that generates a superposition of L initial states $\{\mathbf{x}_k\}_{k=0}^{L-1}$ as

$$U_0 |0\rangle|0\rangle = \frac{1}{\sqrt{\sum_k \|\mathbf{x}_k\|^2}} \sum_{k=0}^{L-1} |\mathbf{x}_k\rangle |k\rangle. \quad (4)$$

We also introduce a block encoding of matrix \mathbf{A} , which is a unitary operator $U_{\mathbf{A}}$ that satisfies

$$U_{\mathbf{A}} |\mathbf{x}\rangle|0\rangle_{\mathbf{a}} = \omega^{-1} |\mathbf{A}\mathbf{x}\rangle|0\rangle_{\mathbf{a}} + |\perp\rangle \quad (5)$$

for an arbitrary N -dimensional vector \mathbf{x} . Here, $|\cdot\rangle_{\mathbf{a}}$ denotes a ket of an ancilla register, ω is a rescaling factor, and $(I \otimes |0\rangle_{\mathbf{a}}\langle 0|_{\mathbf{a}})|\perp\rangle = 0$. We further assume that the computational costs of these operators are $O(\text{poly log } NL)$. Using U_0 and $U_{\mathbf{A}}$, we prepare a quantum state proportional to $|\mathbf{X}\rangle$ via a QLDES [11, 14, 15]. The ket $|\mathbf{X}\rangle$ is given by

$$|\mathbf{X}\rangle = \sum_{k=0}^{L-1} \sum_{t=0}^{T-1} |\mathbf{x}_k(t)\rangle_1 |k\rangle_2 |t\rangle_3, \quad (6)$$

where $\mathbf{x}_k(t)$ denotes the state at the t -th time step of the trajectory initiated from \mathbf{x}_k . The first register encodes states of the dynamical system, and the second and third

registers—indicating the initial condition k and the time step count t —collectively label the column index of \mathbf{X} as $|kT + t\rangle_{23} = |k\rangle_2 |t\rangle_3$. The gate complexity of the QLDES is $O(T \text{ poly log}(NM/\epsilon))$ for tolerant simulation error ϵ .

Next, a quantum state encoding \mathbf{X}' is prepared by one-time-step simulation of $\dot{\mathbf{x}} = \mathbf{A}\mathbf{x}$ by the QLDES. By treating the M columns of \mathbf{X} as initial states and adding a qubit as the fourth register to indicate the time step count, the QLDES computes a quantum state proportional to

$$|[\mathbf{X} \ \mathbf{X}']\rangle = |\mathbf{X}\rangle|0\rangle_4 + |\mathbf{X}'\rangle|1\rangle_4 \quad (7)$$

with gate complexity $O(\text{poly log}(NM/\epsilon))^4$. This ket vector can be viewed as encoding $[\mathbf{X} \ \mathbf{X}']$, regarding the second to fourth registers as indicating the column index collectively. Measuring the fourth register, we obtain a quantum state $|\hat{\mathbf{X}}\rangle$ or $|\hat{\mathbf{X}}'\rangle$.

B. Step 2

According to the procedure proposed by Schuld et al. [9], we perform the SVD of a normalized matrix $\hat{\mathbf{Z}}$ ($\mathbf{Z} = \mathbf{X}, \mathbf{X}'$, or $[\mathbf{X} \ \mathbf{X}']$) on a quantum computer using C copies of $|\hat{\mathbf{Z}}\rangle$ as

$$|\hat{\mathbf{Z}}\rangle^{\otimes C} \mapsto |\text{SVD}(\hat{\mathbf{Z}})\rangle \approx \sum_{r=1}^R \hat{\sigma}_r^Z |\mathbf{u}_r^Z\rangle |\mathbf{v}_r^{Z*}\rangle |(\hat{\sigma}_r^Z)^2\rangle_5, \quad (8)$$

where $\hat{\sigma}_r^Z := \sigma_r^Z = \sigma_r^Z/\|\mathbf{Z}\|_F$, and $|(\hat{\sigma}_r^Z)^2\rangle_5$ designates the computational basis of the extra fifth register indicating the binary representation of $(\hat{\sigma}_r^Z)^2$. Note that matrix normalization does not change singular vectors: $\mathbf{u}_r^{\hat{\mathbf{Z}}} = \mathbf{u}_r^Z$ and $\mathbf{v}_r^{\hat{\mathbf{Z}}} = \mathbf{v}_r^Z$. Thus we omit the hat ($\hat{\cdot}$) in the superscript of singular vectors for brevity. This quantum SVD process utilizes density matrix exponentiation [4] and quantum phase estimation. The necessary number of state copies C for precision ϵ is $O(1/\epsilon^2)$ [28].

C. Step 3

The estimation of $\tilde{\mathbf{K}}'$ is based on the following factorization:

$$\tilde{\mathbf{K}}' \approx \frac{\|\mathbf{X}'\|_F}{\|\mathbf{X}\|_F} (\mathbf{Q}^\dagger \mathbf{U}') \hat{\Sigma}' (\mathbf{V}'^\dagger \mathbf{V}) \hat{\Sigma}^{-1} (\mathbf{U}^\dagger \mathbf{Q}), \quad (9)$$

⁴ In the one-step simulation, access to a unitary oracle that generates the initial states $|\hat{\mathbf{X}}\rangle$ is not available; however we can still prepare multiple copies of $|\hat{\mathbf{X}}\rangle$. In this situation, we may not be able to apply the amplitude amplification protocol [7] to reduce the complexity with respect to the condition number of an underlying linear system in the QLDES routine. The condition number is $\tilde{O}(T \sup_{t \in [0, T-1]} \|\exp(t\mathbf{A})\|_2)$ [14, 15], which is $O(1)$ for the one-step simulation. Therefore, the inaccessibility of the quantum oracle generating $|\hat{\mathbf{X}}\rangle$ should not be a critical issue.

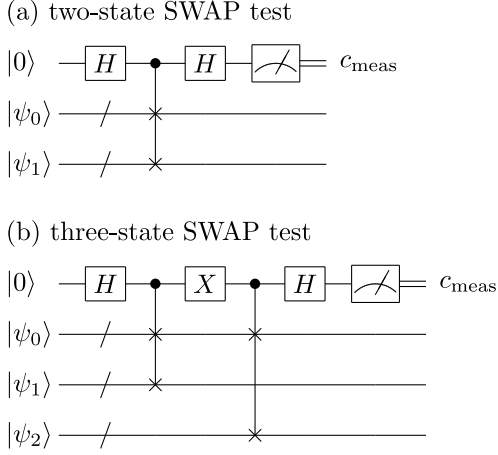


FIG. 1. Quantum circuit for inner product estimation using controlled SWAP gates. The input states $|\psi_k\rangle$ ($k = 0, 1, 2$) are arbitrary quantum states. (a) In the two-state SWAP test, $\Pr[c_{\text{meas}} = 0] - \Pr[c_{\text{meas}} = 1] = |\langle\psi_0|\psi_1\rangle|^2$. (b) In the three-state SWAP test, $\Pr[c_{\text{meas}} = 0] - \Pr[c_{\text{meas}} = 1] = \text{Re}(\langle\psi_0|\psi_1\rangle\langle\psi_1|\psi_2\rangle\langle\psi_2|\psi_0\rangle)$. When a phase gate S is applied to the first qubit just after the first Hadamard gate, $\Pr[c_{\text{meas}} = 0] - \Pr[c_{\text{meas}} = 1] = \text{Im}(\langle\psi_0|\psi_1\rangle\langle\psi_1|\psi_2\rangle\langle\psi_2|\psi_0\rangle)$.

where $\hat{\mathbf{X}} \approx \mathbf{U}\hat{\Sigma}\mathbf{V}^\dagger$ and $\hat{\mathbf{X}}' \approx \mathbf{U}'\hat{\Sigma}'\mathbf{V}'^\dagger$ are the SVDs of the normalized data matrices with rank- R truncation. The first factor $\|\mathbf{X}'\|_{\text{F}}/\|\mathbf{X}\|_{\text{F}}$ ($= \|\mathbf{X}'\|/\|\mathbf{X}\|$) can be estimated by measuring the fourth register of $|\mathbf{X}\mathbf{X}'\rangle$ because the probability ratio of measured values 1 to 0 equals the square of this factor. The diagonal elements of $\hat{\Sigma}$ and $\hat{\Sigma}'$, i.e., $\{\hat{\sigma}_r^{\mathbf{X}}\}_{r=1}^R$ and $\{\hat{\sigma}_r^{\mathbf{X}'}\}_{r=1}^R$, can be estimated by measuring the fifth register of $|\text{SVD}(\hat{\mathbf{X}})\rangle$ and $|\text{SVD}(\hat{\mathbf{X}}')\rangle$. All the off-diagonal elements of $\hat{\Sigma}$ and $\hat{\Sigma}'$ are zero. The elements of matrices $\mathbf{Q}^\dagger\mathbf{U}'$, $\mathbf{U}^\dagger\mathbf{Q}$, and $\mathbf{V}'^\dagger\mathbf{V}$ are inner products between singular vectors. Note that the r -th column vector of \mathbf{Q} corresponds to $\mathbf{u}_r^{[\mathbf{X}\mathbf{X}']}$. Now, the remaining task is to estimate $\langle\mathbf{u}_r^{[\mathbf{X}\mathbf{X}']}|\mathbf{u}_{r'}^{\mathbf{X}'}\rangle$, $\langle\mathbf{u}_r^{\mathbf{X}}|\mathbf{u}_{r'}^{[\mathbf{X}\mathbf{X}']}\rangle$, and $\langle\mathbf{v}_r^{\mathbf{X}'}|\mathbf{v}_{r'}^{\mathbf{X}}\rangle$ for R^2 combinations of r and r' .

The two-state SWAP test depicted in Fig. 1(a) is often employed for estimating the absolute value of the inner product between arbitrary quantum states $|\psi_0\rangle$ and $|\psi_1\rangle$. However, the two-state SWAP test cannot estimate the phase (argument) of the inner product. Furthermore, the global phase of a singular vector is arbitrary. For instance, if we have a singular vector pair ($|\mathbf{u}_r\rangle, |\mathbf{v}_r^*\rangle$), then $(e^{i\theta}|\mathbf{u}_r\rangle, e^{-i\theta}|\mathbf{v}_r^*\rangle)$ is also a valid pair, where θ ranges from 0 to 2π . The choice of the global phase of the singular vector pair changes inner products to be estimated. To overcome these challenges, we introduce the *three-*

state SWAP test (Fig. 1(b)) and *reference states* for the left and right singular vectors.

First, we estimate the inner products between left singular vectors. We define the global phase of each left singular vector state $|\mathbf{u}\rangle$ such that $\arg\langle\chi_1|\mathbf{u}\rangle = 0$ for a fixed reference quantum state $|\chi_1\rangle$. The choice of $|\chi_1\rangle$ is arbitrary⁵, provided that $\langle\chi_1|\mathbf{u}\rangle \neq 0$ for all relevant left singular vectors \mathbf{u} and that it can be prepared with $O(\text{poly log } N)$ complexity by a unitary gate as $U_{\chi_1}|0\rangle = |\chi_1\rangle$. The two-state SWAP test between $|\chi_1\rangle$ and $|\mathbf{u}\rangle$ estimates $|\langle\chi_1|\mathbf{u}\rangle|$. Here, the singular vector state $|\mathbf{u}\rangle$ can be prepared by executing the quantum SVD and measuring the fifth register encoding squared singular values. Additionally, the three-state SWAP test between $|\chi_1\rangle$ and arbitrary left singular vector states $|\mathbf{u}\rangle$ and $|\mathbf{u}'\rangle$ provides an estimate of $\langle\chi_1|\mathbf{u}\rangle\langle\mathbf{u}'|\chi_1\rangle$. Leveraging the known absolute values and phases of $\langle\chi_1|\mathbf{u}\rangle$ and $\langle\mathbf{u}'|\chi_1\rangle$, we can derive an estimate of $\langle\mathbf{u}|\mathbf{u}'\rangle$. In this way, $\langle\mathbf{u}_r^{[\mathbf{X}\mathbf{X}']}|\mathbf{u}_{r'}^{\mathbf{X}'}\rangle$ and $\langle\mathbf{u}_r^{\mathbf{X}}|\mathbf{u}_{r'}^{[\mathbf{X}\mathbf{X}']}\rangle$ can be estimated.

Next, we estimate the inner products between right singular vectors. As with $|\chi_1\rangle$, a reference state $|\chi_2\rangle$ for right singular vectors can be chosen arbitrarily⁵, provided that $\langle\chi_2|\mathbf{v}^*\rangle \neq 0$ for all relevant right singular vectors \mathbf{v} and that it can be prepared with $O(\text{poly log } N)$ complexity by a unitary gate as $U_{\chi_2}|0\rangle = |\chi_2\rangle$. Since the global phase of a right singular vector is synchronized with its corresponding left singular vector, we cannot arbitrarily define $\arg\langle\chi_2|\mathbf{v}^*\rangle$; instead, we need to estimate it as well. Once we determine $\langle\chi_2|\mathbf{v}^*\rangle$ for every right singular vector \mathbf{v} , we can estimate $\langle\mathbf{v}_r^{\mathbf{X}'}|\mathbf{v}_{r'}^{\mathbf{X}}\rangle$ using the three-state SWAP test as described above. Thus, let us consider how to determine $\langle\chi_2|\mathbf{v}^*\rangle$. We employ the quantum circuit shown in Fig. 2 for this inner product estimation. The input state to this circuit is prepared according to the following protocol:

1. Initialize the first to fifth registers as in steps 1 and 2 of the qDMD algorithm. Additionally, append a sixth register initialized with a single qubit in the state $(|0\rangle_6 + |1\rangle_6)/\sqrt{2}$.
2. Perform linear differential equation simulation to create $|\mathbf{X}\hat{\mathbf{X}}'\rangle$, conditioned on the sixth register being zero.
3. Perform the quantum SVD of $\hat{\mathbf{X}}$, conditioned on both the fourth and sixth registers being zero.
4. Apply the unitary gates that create the reference states as $(U_{\chi_1} \otimes U_{\chi_2})|0\rangle_1|0\rangle_{23} = |\chi_1\rangle_1|\chi_2\rangle_{23}$, conditioned on the sixth register being one.

This protocol yields the quantum state given by

⁵ However, the choice of $|\chi_1\rangle$ and $|\chi_2\rangle$ affects the algorithm's effi-

ciency (see Supplemental Material).

$$\frac{1}{\sqrt{2}\|\mathbf{X}\ \mathbf{X}'\|_{\text{F}}} \left[\|\mathbf{X}\|_{\text{F}} \sum_{r=1}^R \hat{\sigma}_r^{\mathbf{X}} |\mathbf{u}_r^{\mathbf{X}}\rangle_1 |\mathbf{v}_r^{\mathbf{X}*}\rangle_{23} |0\rangle_4 |(\hat{\sigma}_r^{\mathbf{X}})^2\rangle_5 + |\mathbf{X}'\rangle_{123} |1\rangle_4 |0\rangle_5 \right] |0\rangle_6 + \frac{1}{\sqrt{2}} |\chi_1\rangle_1 |\chi_2\rangle_{23} |0\rangle_4 |0\rangle_5 |1\rangle_6. \quad (10)$$

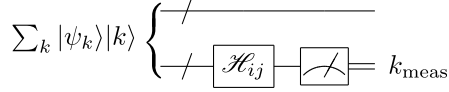


FIG. 2. Quantum circuit for inner product estimation using a Hadamard gate. The $|\psi_k\rangle$'s are arbitrary ket vectors that satisfy $\sum_k \|\psi_k\|^2 = 1$. Gate \mathcal{H}_{ij} is defined by $H_{ij} + I_{ij}^{\dagger}$. Here, H_{ij} is the Hadamard gate on the 2-dimensional Hilbert space $\mathcal{H} := \text{span}\{|i\rangle, |j\rangle\}$, i.e., $H_{ij} := (|i\rangle\langle i| + |i\rangle\langle j| + |j\rangle\langle i| - |j\rangle\langle j|)/\sqrt{2}$, and I_{ij}^{\dagger} is the identity operator on the orthogonal complementary space of \mathcal{H} . The measurement probability satisfies $\Pr[k_{\text{meas}} = i] - \Pr[k_{\text{meas}} = j] = 2 \text{Re} \langle \psi_i | \psi_j \rangle$. When the phase shift $|j\rangle \mapsto -i|j\rangle$ is applied before \mathcal{H}_{ij} , $\Pr[k_{\text{meas}} = i] - \Pr[k_{\text{meas}} = j] = 2 \text{Im} \langle \psi_i | \psi_j \rangle$.

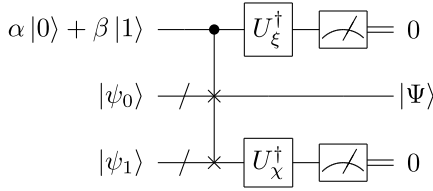


FIG. 3. Quantum circuit for coherent addition of two quantum states $|\psi_0\rangle$ and $|\psi_1\rangle$ [29]. U_x is a unitary gate satisfying $U_x |0\rangle = |\chi\rangle$. U_ξ is a unitary gate satisfying $U_\xi |0\rangle = |\xi\rangle$, where $|\xi\rangle := \sqrt{c_0/(c_0 + c_1)} |0\rangle + \sqrt{c_1/(c_0 + c_1)} |1\rangle$. If the measured values of the first and third registers are both zero, the coherent addition has been successful.

Let us set $|0\rangle_4 |0\rangle_5 |1\rangle_6$ and $|0\rangle_4 |(\hat{\sigma}_r^{\mathbf{X}})^2\rangle_5 |0\rangle_6$ to $|i\rangle$ and $|j\rangle$ in the circuit diagram shown in Fig. 2, respectively. Then, the circuit provides an estimate of $\langle \chi_1 | \mathbf{u}_r^{\mathbf{X}} \rangle \langle \chi_2 | \mathbf{v}_r^{\mathbf{X}*} \rangle$. Since we know the value of $\langle \chi_1 | \mathbf{u}_r^{\mathbf{X}} \rangle$, we can derive an estimate of $\langle \chi_2 | \mathbf{v}_r^{\mathbf{X}*} \rangle$. Similarly, we can estimate $\langle \chi_2 | \mathbf{v}_r^{\mathbf{X}*} \rangle$ by performing the quantum SVD of \mathbf{X}' , conditioned on the fourth register being one instead of zero, in the third step of the above protocol.

The number of quantum SVDs necessary for estimating $\tilde{\mathbf{K}}'$ with precision ϵ is $O(1/\epsilon^2 \text{poly } R)$, excluding reference state preparation costs. The factor $O(1/\epsilon^2)$ originates from sampling errors obeying the central limit theorem. While preparing the reference states may require additional quantum SVDs, the overall gate complexity remains at $O(\text{poly log } N)$. A detailed analysis of the computational complexity can be found in Supplemental Material.

D. Step 5

A quantum state encoding the r -th DMD mode is given by

$$|\tilde{\mathbf{w}}_r\rangle \approx \sum_{r'=1}^R \tilde{w}_r^{r'} |\mathbf{u}_{r'}^{[\mathbf{X}\ \mathbf{X}']}\rangle, \quad (11)$$

where $\tilde{\mathbf{w}}_r' = (\tilde{w}_r^{r'1}, \dots, \tilde{w}_r^{r'R})^\top$ is computed at step 4. Such a coherent superposition of quantum states can be created using the quantum circuit shown in Fig. 3. This circuit creates a superposition of $|\psi_0\rangle$ and $|\psi_1\rangle$ [29]:

$$|\Psi\rangle = \alpha \frac{\langle \chi | \psi_1 \rangle}{|\langle \chi | \psi_1 \rangle|} |\psi_0\rangle + \beta \frac{\langle \chi | \psi_0 \rangle}{|\langle \chi | \psi_0 \rangle|} |\psi_1\rangle. \quad (12)$$

Here, α and β are user-specified complex amplitudes, and $|\chi\rangle$ is a reference quantum state. This addition process is probabilistic. The success probability is $c_0 c_1 / (c_0 + c_1)$ if $\langle \psi_0 | \psi_1 \rangle = 0$, where $c_i = |\langle \chi | \psi_i \rangle|^2$. By recursively creating coherent superpositions of two states, we can construct the multi-state superposition $|\tilde{\mathbf{w}}_r\rangle$ with $O(\text{poly } R)$ times of the quantum SVD (see Supplemental Material).

IV. CONCLUSION

The qDMD algorithm performs DMD on quantum time series data generated by a QLDES. This algorithm is also capable of computing (possibly complex) eigenvalues and eigenvectors of matrices. Excluding reference state preparation costs, the total gate complexity scales as $O(T \text{ poly log}(NM/\epsilon) \text{ poly}(R)/\epsilon^4)$. The qDMD algorithm can achieve an exponential speedup over its classical counterpart in terms of N if R remains at most $O(\text{poly log } N)$. Since the algorithm utilizes density matrix exponentiation and sampling-based inner product estimation, the dependency on ϵ is less optimal than that of the classical counterpart. Reducing the complexity with respect to ϵ should be addressed in future work.

ACKNOWLEDGMENTS

This work was supported by JST, PRESTO Grant Number JPMJPR2018, Japan, and partially by ‘‘Crossover Alliance to Create the Future with People, Intelligence and Materials’’ from MEXT, Japan (to YM).

-
- [1] A. Y. Kitaev, Quantum measurements and the Abelian stabilizer problem (1995), arXiv:quant-ph/9511026 [quant-ph].
- [2] R. Cleve, A. Ekert, C. Macchiavello, and M. Mosca, Quantum algorithms revisited, Proceedings of the Royal Society of London. Series A: Mathematical, Physical and Engineering Sciences **454**, 339 (1998).
- [3] D. S. Abrams and S. Lloyd, Quantum algorithm providing exponential speed increase for finding eigenvalues and eigenvectors, Physical Review Letters **83**, 5162 (1999).
- [4] S. Lloyd, M. Mohseni, and P. Rebentrost, Quantum principal component analysis, Nature Physics **10**, 631 (2014).
- [5] P. Rebentrost, A. Steffens, I. Marvian, and S. Lloyd, Quantum singular-value decomposition of nonsparse low-rank matrices, Physical Review A **97**, 012327 (2018).
- [6] A. W. Harrow, A. Hassidim, and S. Lloyd, Quantum algorithm for linear systems of equations, Physical Review Letters **103**, 150502 (2009).
- [7] A. M. Childs, R. Kothari, and R. D. Somma, Quantum algorithm for systems of linear equations with exponentially improved dependence on precision, SIAM Journal on Computing **46**, 1920 (2017).
- [8] A. Aspuru-Guzik, A. D. Dutoi, P. J. Love, and M. Head-Gordon, Simulated quantum computation of molecular energies, Science **309**, 1704 (2005).
- [9] M. Schuld, I. Sinayskiy, and F. Petruccione, Prediction by linear regression on a quantum computer, Physical Review A **94**, 022342 (2016).
- [10] D. W. Berry, High-order quantum algorithm for solving linear differential equations, Journal of Physics A: Mathematical and Theoretical **47**, 105301 (2014).
- [11] D. W. Berry, A. M. Childs, A. Ostrander, and G. Wang, Quantum algorithm for linear differential equations with exponentially improved dependence on precision, Communications in Mathematical Physics **356**, 1057 (2017).
- [12] A. M. Childs and J.-P. Liu, Quantum spectral methods for differential equations, Communications in Mathematical Physics **375**, 1427 (2020).
- [13] J.-P. Liu, H. Ø. Kolden, H. K. Krovi, N. F. Loureiro, K. Trivisa, and A. M. Childs, Efficient quantum algorithm for dissipative nonlinear differential equations, Proceedings of the National Academy of Sciences **118**, e2026805118 (2021).
- [14] H. Krovi, Improved quantum algorithms for linear and nonlinear differential equations, Quantum **7**, 913 (2023).
- [15] D. Jennings, M. Lostaglio, R. B. Lowrie, S. Pallister, and A. T. Sornborger, The cost of solving linear differential equations on a quantum computer: fast-forwarding to explicit resource counts (2024), arXiv:2309.07881 [quant-ph].
- [16] S. L. Brunton, M. Budišić, E. Kaiser, and J. N. Kutz, Modern Koopman theory for dynamical systems, SIAM Review **64**, 229 (2022).
- [17] Y. T. Lin, R. B. Lowrie, D. Aslangil, Y. Subaşı, and A. T. Sornborger, Koopman von Neumann mechanics and the Koopman representation: A perspective on solving nonlinear dynamical systems with quantum computers (2022), arXiv:2202.02188 [quant-ph].
- [18] B. T. Kiani, G. De Palma, D. Englund, W. Kaminsky, M. Marvian, and S. Lloyd, Quantum advantage for differential equation analysis, Physical Review A **105**, 022415 (2022).
- [19] J. H. Tu, C. W. Rowley, D. Luchtenburg, S. L. Brunton, and J. N. Kutz, On dynamic mode decomposition: Theory and applications, Journal of Computational Dynamics **1**, 391 (2014).
- [20] A. Steffens, P. Rebentrost, I. Marvian, J. Eisert, and S. Lloyd, An efficient quantum algorithm for spectral estimation, New Journal of Physics **19**, 033005 (2017).
- [21] C. Xue, Z.-Y. Chen, T.-P. Sun, X.-F. Xu, S.-M. Chen, H.-Y. Liu, X.-N. Zhuang, Y.-C. Wu, and G.-P. Guo, Quantum dynamic mode decomposition algorithm for high-dimensional time series analysis, Intelligent Computing **2**, 0045 (2023).
- [22] A. Teplukhin, B. K. Kendrick, and D. Babikov, Solving complex eigenvalue problems on a quantum annealer with applications to quantum scattering resonances, Physical Chemistry Chemical Physics **22**, 26136 (2020).
- [23] H. Wang, L.-A. Wu, Y.-x. Liu, and F. Nori, Measurement-based quantum phase estimation algorithm for finding eigenvalues of non-unitary matrices, Physical Review A **82**, 062303 (2010).
- [24] A. Daskin, A. Grama, and S. Kais, A universal quantum circuit scheme for finding complex eigenvalues, Quantum Information Processing **13**, 333 (2014).
- [25] C. Shao, Computing eigenvalues of diagonalizable matrices on a quantum computer, ACM Transactions on Quantum Computing **3**, 1 (2022).
- [26] L. N. Trefethen and D. Bau, *Numerical linear algebra* (Society for Industrial and Applied Mathematics, Philadelphia, United States, 1997).
- [27] M. A. Nielsen and I. L. Chuang, *Quantum Computation and Quantum Information* (Cambridge University Press, Cambridge, United Kingdom, 2010).
- [28] S. Kimmel, C. Y.-Y. Lin, G. H. Low, M. Ozols, and T. J. Yoder, Hamiltonian simulation with optimal sample complexity, npj Quantum Information **3**, 13 (2017).
- [29] M. Oszmaniec, A. Grudka, M. Horodecki, and A. Wójcik, Creating a superposition of unknown quantum states, Physical Review Letters **116**, 110403 (2016).

Supplemental Material for “A quantum algorithm for dynamic mode decomposition integrated with a quantum differential equation solver”

Yuta Mizuno^{1,2,3,*} and Tamiki Komatsuzaki^{1,2,3,4}

¹*Research Institute for Electronic Science, Hokkaido University, Sapporo, Hokkaido 001-0020, Japan*

²*Institute for Chemical Reaction Design and Discovery (WPI-ICReDD),
Hokkaido University, Sapporo, Hokkaido 001-0021, Japan*

³*Graduate School of Chemical Sciences and Engineering,
Hokkaido University, Sapporo, Hokkaido 060-8628, Japan*

⁴*SANKEN, Osaka University, Ibaraki, Osaka 567-0047, Japan*

(Dated: April 23, 2024)

CONTENTS

I. Computational Complexity of Estimating $\tilde{\mathbf{K}}'$	1
A. Required number of repetitions of each elemental estimation process	2
B. Required number of quantum SVDs for singular value and vector collection	2
C. Required number of quantum SVDs for estimating $\tilde{\mathbf{K}}'$	4
II. Reference State Preparation for the Inner Product Estimation	5
A. Choice of $ \chi_1\rangle$ and $ \chi_2\rangle$: An example	5
B. Computation of $ \chi_1\rangle$ and $ \chi_2\rangle$: An example	8
C. Summary and concluding remarks	12
III. Computing DMD Mode States	12
A. Recursive coherent state addition	12
B. Computational complexity	14
C. Reference state preparation	15
IV. Comparison of the qDMD and Related Algorithms	18
A. Time Series Analysis Algorithms	18
B. Quantum Eigensolvers for Complex Eigenvalue Problems	19
V. Dynamic Mode Decomposition for Defective Systems	20
References	21

I. COMPUTATIONAL COMPLEXITY OF ESTIMATING $\tilde{\mathbf{K}}'$

This section offers a detailed analysis of the computational complexity involved in estimating $\tilde{\mathbf{K}}'$. We assume that the required precision of each element of $\tilde{\mathbf{K}}'$ is ϵ in this section. Note that we omit the discussion on the computational complexity of preparing reference states for the inner product estimation, which will be presented in the next section.

In what follows, we first evaluate the required number of repetitions of each elemental estimation process, such as the three-state SWAP test for estimating an inner product. Next, we evaluate the required number of quantum SVDs for collecting singular values and their associated singular vector states necessary for the singular value estimation and the two-state and three-state SWAP tests. A single quantum SVD process yields a quantum state $|\text{SVD}(\hat{\mathbf{Z}})\rangle$ and the measurement of the fifth register encoding singular values provides a triple of a singular value and its associated left and right singular vector states *at random*. Therefore, we need to take into account this probabilistic nature to estimate the required number of quantum SVDs. To this end, we introduce a general theorem on the necessary number of trials of random selection, proven by Brayton [1]. Finally, we evaluate the total number of quantum SVDs necessary for estimating the whole matrix $\tilde{\mathbf{K}}'$ as well as its gate complexity.

* mizuno@es.hokudai.ac.jp

TABLE SI. Summary of the elemental estimation processes in estimating $\tilde{\mathbf{K}}'$.

Estimation Target	Input State(s)	Estimation Method	Required Number of Repetitions
$\frac{\ \mathbf{X}'\ _F}{\ \mathbf{X}\ _F}$	$ \llbracket[\mathbf{X} \ \mathbf{X}']\rrbracket_{1:4}\rangle$	Measuring the 4th register	$O\left(\frac{1}{\epsilon^2}\right)$
$\hat{\sigma}$	$ \hat{\sigma}^2\rangle$	Readout of the bit string of the register	1
$\langle\chi_1 \mathbf{u}\rangle$	$ \chi_1\rangle, \mathbf{u}\rangle$	Two-state SWAP test	$O\left(\frac{1}{\epsilon^2}\right)$
$\langle\mathbf{u} \mathbf{u}'\rangle$	$ \chi_1\rangle, \mathbf{u}\rangle, \mathbf{u}'\rangle$	Three-state SWAP test	$O\left(\frac{1}{ \langle\chi_1 \mathbf{u}\rangle ^2 \langle\chi_1 \mathbf{u}'\rangle ^2\epsilon^2}\right)$
$\langle\mathbf{v} \mathbf{v}'\rangle$	$ \chi_2\rangle, \mathbf{v}^*\rangle, \mathbf{v}'^*\rangle$	Three-state SWAP test	$O\left(\frac{1}{ \langle\chi_2 \mathbf{v}^*\rangle ^2 \langle\chi_2 \mathbf{v}'^*\rangle ^2\epsilon^2}\right)$
$\langle\chi_2 \mathbf{v}_r^{\mathbf{Z}*}\rangle$	$ 0\rangle_{1:5} \frac{ 0\rangle_6 + 1\rangle_6}{\sqrt{2}}$	The process utilizing the circuit shown in Fig. 2 of the main text	$O\left(\frac{1}{P_{\mathbf{Z}}(\hat{\sigma}_r^{\mathbf{Z}})^2 \langle\chi_1 \mathbf{u}_r^{\mathbf{Z}}\rangle ^2\epsilon^2}\right)$

A. Required number of repetitions of each elemental estimation process

Table SI summarizes the elemental estimation process and their required numbers of repetitions.

The factor $\|\mathbf{X}'\|_F/\|\mathbf{X}\|_F$ is estimated through the measurement of the fourth register of $|\llbracket[\mathbf{X} \ \mathbf{X}']\rrbracket_{1:4}\rangle$. Here, we denote a ket vector of the k -th to k' -th registers like $|\rangle_{k:k'}$. This estimation relies on the estimation of the probability of measuring zero and the probability of measuring one. The error of the probability estimation decrease as the number of samples increases obeying the central limit theorem. Therefore, $O(1/\epsilon^2)$ repetitions of the estimation process is needed to estimate the factor with precision ϵ .

Each normalized singular value $\hat{\sigma}$ of matrix \mathbf{Z} is encoded in the fifth register of $|\text{SVD}(\hat{\mathbf{Z}})\rangle_{1:5}$. Measuring the fifth register, the quantum state of the fifth register collapses into a computational basis state that encodes one of the normalized singular values of \mathbf{Z} as a bit string. Consequently, a single readout of the bit string suffices to estimate the singular value. Note that it is probabilistic which singular value is measured; this probabilistic nature will be considered in the next subsection.

For each left singular vector \mathbf{u} , the inner product $\langle\chi_1|\mathbf{u}\rangle$ is estimated by the two-state SWAP test. The two-state SWAP test estimates the inner product through measurement probability estimation. Thus $O(1/\epsilon^2)$ repetitions of the two-state SWAP test is necessary for estimating $\langle\chi_1|\mathbf{u}\rangle$ with precision ϵ .

For each pair of left singular vectors \mathbf{u} and \mathbf{u}' , the inner product $\langle\mathbf{u}|\mathbf{u}'\rangle$ is estimated by the three-state SWAP test. The three-state SWAP test estimates $\langle\chi_1|\mathbf{u}\rangle\langle\mathbf{u}|\mathbf{u}'\rangle\langle\mathbf{u}'|\chi_1\rangle$. Therefore, the required precision of the three-state SWAP test is $|\langle\chi_1|\mathbf{u}\rangle||\langle\chi_1|\mathbf{u}'\rangle|\epsilon$ for estimating $\langle\mathbf{u}|\mathbf{u}'\rangle$ with precision ϵ . Given that the estimation error obeys the central limit theorem, the required number of the three-state SWAP test for estimating $\langle\mathbf{u}|\mathbf{u}'\rangle$ is $O(1/|\langle\chi_1|\mathbf{u}\rangle|^2|\langle\chi_1|\mathbf{u}'\rangle|^2\epsilon^2)$. Likewise, for each pair of right singular vectors \mathbf{v} and \mathbf{v}' , the estimation of $\langle\mathbf{v}|\mathbf{v}'\rangle$ requires $O(1/|\langle\chi_2|\mathbf{v}^*\rangle|^2|\langle\chi_2|\mathbf{v}'^*\rangle|^2\epsilon^2)$ repetitions of the three-state SWAP test.

For each right singular vector $\mathbf{v}_r^{\mathbf{Z}}$ ($\mathbf{Z} = \mathbf{X}, \mathbf{X}'$, $r = 1, \dots, R$), the inner product $\langle\chi_2|\mathbf{v}_r^{\mathbf{Z}*}\rangle$ is estimated by the process utilizing the circuit depicted in Fig. 2 of the main text. This process estimate $\sqrt{P_{\mathbf{Z}}}\hat{\sigma}_r^{\mathbf{Z}}\langle\chi_1|\mathbf{u}_r^{\mathbf{Z}}\rangle\langle\chi_2|\mathbf{v}_r^{\mathbf{Z}*}\rangle$ through probability estimation. Here, $P_{\mathbf{Z}}$ denotes the probability of obtaining $|\mathbf{Z}\rangle$ by measuring the fourth register of $|\llbracket[\mathbf{X} \ \mathbf{X}']\rrbracket\rangle$, that is,

$$P_{\mathbf{Z}} := \frac{\|\mathbf{Z}\|_F^2}{\|\llbracket[\mathbf{X} \ \mathbf{X}']\rrbracket\|_F^2}. \quad (\text{S1})$$

Consequently, the required number of repetitions of running the process is $O(1/P_{\mathbf{Z}}(\hat{\sigma}_r^{\mathbf{Z}})^2|\langle\chi_1|\mathbf{u}_r^{\mathbf{Z}}\rangle|^2\epsilon^2)$.

B. Required number of quantum SVDs for singular value and vector collection

The singular value estimation and the two-state and three-state SWAP tests require quantum states encoding a singular value or a singular vector. Furthermore, it is necessary to repeat the SWAP test for each element a certain number of times, as discussed in the previous subsection. A single quantum SVD process and measuring the fifth register provides a triple of a singular value and its associated left and right singular vector states at random. Thus, in this subsection, let us consider the number of quantum SVDs necessary for collecting m each of all dominant singular value and singular vector states.

Brayton [1] investigated the asymptotic behavior of the expected number of trials necessary to collect m copies of a set of n objects by random selection, denoted by $E_m(n)$. The probability of selecting the i -th object is assumed to be given by

$$p_i = \int_{(i-1)/n}^{i/n} f(s) ds, \quad (\text{S2})$$

where the function f satisfies the following conditions:

1. $\int_0^1 f(s) ds = 1$.
2. $\min f(s) = \delta > 0$; $\max f(s) < \infty$.
3. $f(s)$ is a function of bounded variation on $[0, 1]$.

Brayton proved that if $f(s) = \delta$ on a set of intervals of length $l > 0$, the asymptotic behavior of $E_m(n)$ as $n \rightarrow \infty$ is given by

$$E_m(n) = \frac{n}{\delta} \left[\log \Gamma n + (m-1) \log \log \Gamma n + \gamma + (m-1) \log \frac{1}{\delta} + o(1) \right], \quad (\text{S3})$$

where γ is the Euler–Mascheroni constant and

$$\Gamma = l \frac{\delta^{m-1}}{(m-1)!}. \quad (\text{S4})$$

Let us define f by a piecewise constant function such that $f(s) = np_i$ for $(i-1)/n \leq s < i/n$. Additionally, we denote the minimum probability of random selection by p_{\min} . In that case, $\delta = np_{\min} \leq 1$ and $\Gamma \leq l \leq 1$. Therefore, the expected number of necessary trials roughly scales as

$$E_m(n) = O \left(\frac{1}{p_{\min}} \left[\log n + (m-1) \log \frac{\log n}{np_{\min}} \right] \right). \quad (\text{S5})$$

We can further rewrite this asymptotic equation using the maximum probability of random selection, p_{\max} , as

$$E_m(n) = O \left(\frac{p_{\max}}{p_{\min}} \left[n \log n + n(m-1) \log \left(\frac{p_{\max}}{p_{\min}} \log n \right) \right] \right), \quad (\text{S6})$$

because $1 \leq np_{\max}$ holds.

In the case of the singular value and singular vector collection for matrix \mathbf{Z} , the number of objects n equals R , and the ratio of the maximum and minimum probabilities is given by

$$\frac{p_{\max}}{p_{\min}} = \frac{\max_r (\hat{\sigma}_r^{\mathbf{Z}})^2}{\min_r (\hat{\sigma}_r^{\mathbf{Z}})^2} = \left(\frac{\max_r \hat{\sigma}_r^{\mathbf{Z}}}{\min_r \hat{\sigma}_r^{\mathbf{Z}}} \right)^2. \quad (\text{S7})$$

Let us define a parameter $\kappa_{\mathbf{Z}}$ as

$$\kappa_{\mathbf{Z}} := \frac{\max_r \sigma_r^{\mathbf{Z}}}{\min_r \sigma_r^{\mathbf{Z}}} = \frac{\max_r \hat{\sigma}_r^{\mathbf{Z}}}{\min_r \hat{\sigma}_r^{\mathbf{Z}}}. \quad (\text{S8})$$

The parameter $\kappa_{\mathbf{Z}}$ is also known as the condition number of \mathbf{Z} (with rank- R truncation). Using this parameter, we can write the required number of quantum SVDs for collecting m each of all dominant singular value and singular vector states of \mathbf{Z} as

$$E_m(R) = O \left(\kappa_{\mathbf{Z}}^2 \left[R \log R + (m-1) R \log (\kappa_{\mathbf{Z}}^2 \log R) \right] \right). \quad (\text{S9})$$

Note that since the qDMD algorithm relies on the rank- R approximation of $\hat{\mathbf{Z}}$, the probability of selecting a singular value other than the R dominant singular values may be non-zero. However, as we determine R such that the error of the rank- R approximation is less than a specified tolerance in terms of the Frobenius norm, the probability of selecting one of R dominant singular values, given by $\sum_{r=1}^R (\hat{\sigma}_r^{\mathbf{Z}})^2$, is $O(1)$. Thus we can neglect the probability of selecting other minor singular values.

C. Required number of quantum SVDs for estimating $\tilde{\mathbf{K}}'$

Now, we evaluate the total number of quantum SVDs necessary for estimating the whole matrix $\tilde{\mathbf{K}}'$. We first note that the factor $\|\mathbf{X}'\|_{\text{F}}/\|\mathbf{X}\|_{\text{F}}$ and the normalized singular value matrices $\tilde{\Sigma}$ and $\tilde{\Sigma}'$ can be estimated in the course of preparing singular vector states for the SWAP tests. In other words, we can include the costs of these estimations into those of preparing singular vector states. Therefore, we only consider the computational costs for the inner product estimation.

According to Table SI, the required number of repetitions of the three-state SWAP test depends on inner products between singular vector states and reference states. For the simplicity of the notation, let us introduce a parameter ζ defined as

$$\zeta := \min\{\zeta_1, \zeta_2\}, \quad (\text{S10})$$

$$\zeta_1 := \min \{ |\langle \chi_1 | \mathbf{u}_r^{\mathbf{Z}} \rangle|^2 \mid \mathbf{Z} \in \{\mathbf{X}, \mathbf{X}', [\mathbf{X} \ \mathbf{X}']\}, r \in \{1, \dots, R\} \}, \quad (\text{S11})$$

$$\zeta_2 := \min \{ |\langle \chi_2 | \mathbf{v}_r^{\mathbf{Z}^*} \rangle|^2 \mid \mathbf{Z} \in \{\mathbf{X}, \mathbf{X}'\}, r \in \{1, \dots, R\} \}. \quad (\text{S12})$$

Then, the required number of repetitions of the three-state SWAP test scales as $O(1/(\zeta\epsilon)^2)$. In addition, each singular vector is involved in $O(R)$ different inner products to be estimated by the three-state SWAP test. Consequently, the three-state SWAP test requires $O(R/(\zeta\epsilon)^2)$ copies of each singular vector state in total. Furthermore, the two-state SWAP test requires $O(1/\epsilon^2)$ copies of each left singular vector state. Because $R/\zeta^2 \geq 1$, the total copy number of each singular vector state necessary for the two-state and three-state SWAP tests is roughly estimated as $O(R/(\zeta\epsilon)^2)$. Due to Eq. (S9), we get the order estimate of the total number of quantum SVDs necessary for the SWAP tests in the qDMD algorithm:

$$O\left(\left(\frac{\kappa R}{\zeta\epsilon}\right)^2 \log(\kappa^2 \log R)\right), \quad (\text{S13})$$

where we define κ by $\max_{\mathbf{Z}} \kappa_{\mathbf{Z}}$ for brevity.

According to Table SI, the total number of repetitions of the quantum process for estimating $2R$ inner products $\{\langle \chi_2 | \mathbf{v}_r^{\mathbf{Z}^*} \rangle\}$ is

$$O\left(\frac{\eta}{\zeta_1} \left(\frac{\kappa R}{\epsilon}\right)^2\right), \quad (\text{S14})$$

where we define parameter η as

$$\eta := \frac{1}{\min\{P_{\mathbf{X}}, P_{\mathbf{X}'}\}}, \quad (\text{S15})$$

and we use the equation

$$\frac{1}{\min_r (\hat{\sigma}_r^{\mathbf{Z}})^2} = O(R\kappa_{\mathbf{Z}}^2). \quad (\text{S16})$$

Eq. (S16) is equivalent to the equation $1/p_{\min} \leq R(p_{\max}/p_{\min})$, which is used to derive Eq. (S9) in the previous subsection. Since the process contains one quantum SVD process, this total number of repetitions given by Eq. (S14) equals the total number of quantum SVDs for estimating $\{\langle \chi_2 | \mathbf{v}_r^{\mathbf{Z}^*} \rangle\}$. Additionally, we note that η is $O(1)$ due to the following reason: As stated in the main text, it is assumed that $\Delta t \leq 1/\|\mathbf{A}\|_2$. Hence, the norm change of a state vector due to the one-step time evolution is bounded as follows:

$$\|\mathbf{x}'_j\|_2 \approx \|\mathbf{e}^{\Delta t \mathbf{A}} \mathbf{x}_j\|_2 \leq e^{\Delta t \|\mathbf{A}\|_2} \|\mathbf{x}_j\|_2 \leq e \|\mathbf{x}_j\|_2, \quad (\text{S17})$$

and

$$\|\mathbf{x}_j\|_2 \approx \|\mathbf{e}^{-\Delta t \mathbf{A}} \mathbf{x}'_j\|_2 \leq e^{\Delta t \|\mathbf{A}\|_2} \|\mathbf{x}'_j\|_2 \leq e \|\mathbf{x}'_j\|_2. \quad (\text{S18})$$

Since $\|\mathbf{X}\|_{\text{F}} = \sqrt{\sum_{j=0}^{M-1} \|\mathbf{x}_j\|_2^2}$ and $\|\mathbf{X}'\|_{\text{F}} = \sqrt{\sum_{j=0}^{M-1} \|\mathbf{x}'_j\|_2^2}$, we obtain the inequality

$$\frac{1}{e} \|\mathbf{X}\|_{\text{F}} \lesssim \|\mathbf{X}'\|_{\text{F}} \lesssim e \|\mathbf{X}\|_{\text{F}}. \quad (\text{S19})$$

This implies that $P_{\mathbf{X}}$ and $P_{\mathbf{X}'}$ are $\Omega(1)$, where the Ω -symbol signifies an asymptotic lower bound. Therefore, η is $O(1)$. Due to the facts that $\eta = O(1)$ and that $\zeta \leq \zeta_1 < 1$, the cost estimate in Eq. (S14) is less than that in Eq. (S13).

In summary, the number of quantum SVDs necessary for estimating $\tilde{\mathbf{K}}'$ with precision ϵ is

$$O\left(\left(\frac{\kappa R}{\zeta \epsilon}\right)^2 \log(\kappa^2 \log R)\right). \quad (\text{S20})$$

Because one quantum SVD process requires $O(1/\epsilon^2)$ copies of a data matrix [2], the required number of differential equation solutions is

$$O\left(\frac{1}{\epsilon^4} \left(\frac{\kappa R}{\zeta}\right)^2 \log(\kappa^2 \log R)\right). \quad (\text{S21})$$

The gate complexity is larger than the required number of differential equation solutions by a factor of T poly $\log(NM/\epsilon)$.

II. REFERENCE STATE PREPARATION FOR THE INNER PRODUCT ESTIMATION

One may use any reference states $|\chi_1\rangle$ and $|\chi_2\rangle$, provided that $\langle \chi_1 | \mathbf{u} \rangle \neq 0$ and $\langle \chi_2 | \mathbf{v}^* \rangle \neq 0$ for all relevant left and right singular vectors \mathbf{u} and \mathbf{v} . This condition is the necessary and sufficient condition so that the inner product estimation through the three-state SWAP test is possible. Regardless of the choice of $|\chi_1\rangle$ and $|\chi_2\rangle$, estimates of $\tilde{\mathbf{K}}'$ are identical within a tolerant error. However, the choice of $|\chi_1\rangle$ and $|\chi_2\rangle$ affects the algorithm's efficiency: the computational complexity of estimating $\tilde{\mathbf{K}}'$ is influenced by the choice of $|\chi_1\rangle$ and $|\chi_2\rangle$ through the parameter ζ , as discussed in the previous section; the larger ζ is, the smaller the required number of quantum SVDs is. Moreover, if the reference state preparation has a runtime greater than $O(\text{poly } \log N)$, the qDMD algorithm cannot achieve an exponential speedup with respect to N in total.

In this section, we present an example of quantum procedures preparing $|\chi_1\rangle$ and $|\chi_2\rangle$. The quantum circuits of these procedures can be constructed and executed in $O(\text{poly } \log N)$ time, ensuring that $1/\zeta = O(\text{poly } R)$. Therefore, this example theoretically guarantees that the qDMD algorithm achieves an exponential speedup with respect to N in estimating $\tilde{\mathbf{K}}'$. Additionally, we remark on other possible methods of the reference state preparation at the end of this section.

A. Choice of $|\chi_1\rangle$ and $|\chi_2\rangle$: An example

We define $|\chi_1\rangle$ such that $1/\zeta_1 = O(\text{poly } R)$. Specifically, it is designed here to satisfy the following conditions:

$$|\langle \chi_1 | \mathbf{u}_r^{[\mathbf{X} \ \mathbf{X}']} \rangle|^2 = \Omega\left(\frac{1}{R}\right), \quad (\text{S22})$$

$$|\langle \chi_1 | \mathbf{u}_r^{\mathbf{X}} \rangle|^2 = \Omega\left(\frac{1}{R^2}\right), \quad (\text{S23})$$

$$|\langle \chi_1 | \mathbf{u}_r^{\mathbf{X}'} \rangle|^2 = \Omega\left(\frac{1}{R^3}\right), \quad (\text{S24})$$

for any $r \in \{1, 2, \dots, R\}$. Here, the Ω -symbol signifies an asymptotic lower bound.

Initially, we construct a quantum state $|\chi_1^{(0)}\rangle$ such that $|\langle \chi_1^{(0)} | \mathbf{u}_r^{[\mathbf{X} \ \mathbf{X}']} \rangle|^2 = \Omega(1/R)$ for any $r \in \{1, 2, \dots, R\}$. The superposition of all left singular vector states of $[\mathbf{X} \ \mathbf{X}']$ with equal weights satisfies this condition. Thus we define $|\chi_1^{(0)}\rangle$ as

$$|\chi_1^{(0)}\rangle := \frac{1}{\sqrt{R}} \sum_{r=1}^R |\mathbf{u}_r^{[\mathbf{X} \ \mathbf{X}']} \rangle. \quad (\text{S25})$$

Next, we modify $|\chi_1^{(0)}\rangle$ to a quantum state $|\chi_1^{(1)}\rangle$ that satisfies $|\langle \chi_1^{(1)} | \mathbf{u}_r^{\mathbf{X}} \rangle|^2 = \Omega(1/R^2)$ as well as $|\langle \chi_1^{(1)} | \mathbf{u}_r^{[\mathbf{X} \ \mathbf{X}']} \rangle|^2 = \Omega(1/R)$ for any $r \in \{1, 2, \dots, R\}$. Let $S_1^{(1)}$ be a set of left singular vector states of \mathbf{X} defined by

$$S_1^{(1)} := \left\{ |\mathbf{u}_r^{\mathbf{X}} \rangle \mid r \in \{1, 2, \dots, R\}, |\langle \chi_1^{(0)} | \mathbf{u}_r^{\mathbf{X}} \rangle| \leq \frac{1}{4R} \right\}. \quad (\text{S26})$$

This set is a collection of $|\mathbf{u}_r^{\mathbf{X}}\rangle$ whose overlap with the temporary reference state $|\chi_1^{(0)}\rangle$, i.e., $|\langle\chi_1^{(0)}|\mathbf{u}_r^{\mathbf{X}}\rangle|^2$, is small compared with $1/R^2$. To ensure that $|\mathbf{u}_r^{\mathbf{X}}\rangle \in S_1^{(1)}$ has $\Omega(1/R^2)$ overlap with the reference state, we add a correction term $|\phi_1^{(1)}\rangle$ to the temporary reference state $|\chi_1^{(0)}\rangle$:

$$|\phi_1^{(1)}\rangle := \frac{1}{\sqrt{|S_1^{(1)}|}} \sum_{|\mathbf{u}_r^{\mathbf{X}}\rangle \in S_1^{(1)}} |\mathbf{u}_r^{\mathbf{X}}\rangle, \quad (\text{S27})$$

and

$$|\chi_1^{(1)}\rangle := \mathcal{C}_1^{(1)} \left[|\chi_1^{(0)}\rangle + \frac{1}{2\sqrt{R}} |\phi_1^{(1)}\rangle \right]. \quad (\text{S28})$$

Here, $\mathcal{C}_1^{(1)}$ is the normalizing constant. The coefficient $1/2\sqrt{R}$ of $|\phi_1^{(1)}\rangle$ is introduced to ensure that this correction is small enough not to violate the condition $|\langle\chi_1^{(1)}|\mathbf{u}_r^{[\mathbf{X} \ \mathbf{X}']}\rangle|^2 = \Omega(1/R)$. We can confirm that $|\chi_1^{(1)}\rangle$ satisfies the aforementioned conditions on inner products as follows: The normalizing constant $\mathcal{C}_1^{(1)}$ is $\Omega(1)$ because

$$\begin{aligned} \mathcal{C}_1^{(1)} &= \frac{1}{\| |\chi_1^{(0)}\rangle + \frac{1}{2\sqrt{R}} |\phi_1^{(1)}\rangle \|} \\ &\geq \frac{1}{\| |\chi_1^{(0)}\rangle \| + \frac{1}{2\sqrt{R}} \| |\phi_1^{(1)}\rangle \|} \\ &= \frac{1}{1 + \frac{1}{2\sqrt{R}}} \\ &\geq \frac{2}{3}. \end{aligned} \quad (\text{S29})$$

For any $|\mathbf{u}_r^{[\mathbf{X} \ \mathbf{X}']}\rangle$,

$$\begin{aligned} |\langle\chi_1^{(1)}|\mathbf{u}_r^{[\mathbf{X} \ \mathbf{X}']}\rangle| &\geq \mathcal{C}_1^{(1)} \left[|\langle\chi_1^{(0)}|\mathbf{u}_r^{[\mathbf{X} \ \mathbf{X}']}\rangle| - \frac{1}{2\sqrt{R}} |\langle\phi_1^{(1)}|\mathbf{u}_r^{[\mathbf{X} \ \mathbf{X}']}\rangle| \right] \\ &\geq \frac{2}{3} \left[\frac{1}{\sqrt{R}} - \frac{1}{2\sqrt{R}} \right] \\ &= \frac{1}{3\sqrt{R}}. \end{aligned} \quad (\text{S30})$$

The first inequality follows from the triangle inequality. Likewise, for any $|\mathbf{u}_r^{\mathbf{X}}\rangle \in S_1^{(1)}$,

$$\begin{aligned} |\langle\chi_1^{(1)}|\mathbf{u}_r^{\mathbf{X}}\rangle| &\geq \mathcal{C}_1^{(1)} \left[\frac{1}{2\sqrt{R}} |\langle\phi_1^{(1)}|\mathbf{u}_r^{\mathbf{X}}\rangle| - |\langle\chi_1^{(0)}|\mathbf{u}_r^{\mathbf{X}}\rangle| \right] \\ &\geq \frac{2}{3} \left[\frac{1}{2\sqrt{R}} \frac{1}{\sqrt{|S_1^{(1)}|}} - \frac{1}{4R} \right] \\ &\geq \frac{2}{3} \left[\frac{1}{2\sqrt{R}} \frac{1}{\sqrt{R}} - \frac{1}{4R} \right] \\ &= \frac{1}{6R}. \end{aligned} \quad (\text{S31})$$

Any $|\mathbf{u}_r^{\mathbf{X}}\rangle \notin S_1^{(1)}$ is orthogonal to $|\phi_1^{(1)}\rangle \in \text{span } S_1^{(1)}$. Consequently, for any $|\mathbf{u}_r^{\mathbf{X}}\rangle \notin S_1^{(1)}$,

$$|\langle\chi_1^{(1)}|\mathbf{u}_r^{\mathbf{X}}\rangle| = \mathcal{C}_1^{(1)} |\langle\chi_1^{(0)}|\mathbf{u}_r^{\mathbf{X}}\rangle| \geq \frac{2}{3} \frac{1}{4R} = \frac{1}{6R}. \quad (\text{S32})$$

Therefore, $|\chi_1^{(1)}\rangle$ satisfies $|\langle\chi_1^{(1)}|\mathbf{u}_r^{[\mathbf{X} \ \mathbf{X}']}\rangle|^2 = \Omega(1/R)$ and $|\langle\chi_1^{(1)}|\mathbf{u}_r^{\mathbf{X}}\rangle|^2 = \Omega(1/R^2)$ for any $r \in \{1, 2, \dots, R\}$.

Finally, we modify $|\chi_1^{(1)}\rangle$ to a quantum state $|\chi_1^{(2)}\rangle$ that also satisfies $|\langle\chi_1^{(2)}|\mathbf{u}_r^{\mathbf{X}'}\rangle|^2 = \Omega(1/R^3)$. Let us define $S_1^{(2)}$ as

$$S_1^{(2)} := \left\{ |\mathbf{u}_r^{\mathbf{X}'}\rangle \mid r \in \{1, 2, \dots, R\}, |\langle\chi_1^{(1)}|\mathbf{u}_r^{\mathbf{X}'}\rangle| \leq \frac{1}{14R\sqrt{R}} \right\}. \quad (\text{S33})$$

Then, we define $|\chi_1^{(2)}\rangle$ by adding a correction term $|\phi_1^{(2)}\rangle$ to $|\chi_1^{(1)}\rangle$:

$$|\phi_1^{(2)}\rangle := \frac{1}{\sqrt{|S_1^{(2)}|}} \sum_{|\mathbf{u}_r^{\mathbf{X}'}\rangle \in S_1^{(2)}} |\mathbf{u}_r^{\mathbf{X}'}\rangle, \quad (\text{S34})$$

and

$$|\chi_1^{(2)}\rangle := \mathcal{C}_1^{(2)} \left[|\chi_1^{(1)}\rangle + \frac{1}{7R} |\phi_1^{(2)}\rangle \right], \quad (\text{S35})$$

where $\mathcal{C}_1^{(2)}$ is the normalizing constant. We can confirm that $|\chi_1^{(2)}\rangle$ satisfies the aforementioned conditions on inner products as follows: The normalizing constant $\mathcal{C}_1^{(2)}$ is $\Omega(1)$ because

$$\begin{aligned} \mathcal{C}_1^{(2)} &= \frac{1}{\| |\chi_1^{(1)}\rangle + \frac{1}{7R} |\phi_1^{(2)}\rangle \|} \\ &\geq \frac{1}{\| |\chi_1^{(1)}\rangle \| + \frac{1}{7R} \| |\phi_1^{(2)}\rangle \|} \\ &\geq \frac{1}{1 + \frac{1}{7R}} \\ &\geq \frac{7}{8}. \end{aligned} \quad (\text{S36})$$

For any $|\mathbf{u}_r^{[\mathbf{X} \ \mathbf{X}']}\rangle$,

$$\begin{aligned} |\langle\chi_1^{(2)}|\mathbf{u}_r^{[\mathbf{X} \ \mathbf{X}']}\rangle| &\geq \mathcal{C}_1^{(2)} \left[|\langle\chi_1^{(1)}|\mathbf{u}_r^{[\mathbf{X} \ \mathbf{X}']}\rangle| - \frac{1}{7R} |\langle\phi_1^{(2)}|\mathbf{u}_r^{[\mathbf{X} \ \mathbf{X}']}\rangle| \right] \\ &\geq \frac{7}{8} \left[\frac{1}{3\sqrt{R}} - \frac{1}{7R} \right] \\ &\geq \frac{7}{8} \left[\frac{1}{3\sqrt{R}} - \frac{1}{7\sqrt{R}} \right] \\ &= \frac{1}{6\sqrt{R}}. \end{aligned} \quad (\text{S37})$$

For any $|\mathbf{u}_r^{\mathbf{X}}\rangle$,

$$\begin{aligned} |\langle\chi_1^{(2)}|\mathbf{u}_r^{\mathbf{X}}\rangle| &\geq \mathcal{C}_1^{(2)} \left[|\langle\chi_1^{(1)}|\mathbf{u}_r^{\mathbf{X}}\rangle| - \frac{1}{7R} |\langle\phi_1^{(2)}|\mathbf{u}_r^{\mathbf{X}}\rangle| \right] \\ &\geq \frac{7}{8} \left[\frac{1}{6R} - \frac{1}{7R} \right] \\ &= \frac{1}{48R}. \end{aligned} \quad (\text{S38})$$

For any $|\mathbf{u}_r^{\mathbf{X}'}\rangle \in S_1^{(2)}$,

$$\begin{aligned} |\langle\chi_1^{(2)}|\mathbf{u}_r^{\mathbf{X}'}\rangle| &\geq \mathcal{C}_1^{(2)} \left[\frac{1}{7R} |\langle\phi_1^{(2)}|\mathbf{u}_r^{\mathbf{X}'}\rangle| - |\langle\chi_1^{(1)}|\mathbf{u}_r^{\mathbf{X}'}\rangle| \right] \\ &\geq \frac{7}{8} \left[\frac{1}{7R} \frac{1}{\sqrt{|S_1^{(2)}|}} - \frac{1}{14R\sqrt{R}} \right] \\ &\geq \frac{7}{8} \left[\frac{1}{7R} \frac{1}{\sqrt{R}} - \frac{1}{14R\sqrt{R}} \right] \\ &= \frac{1}{16R\sqrt{R}}. \end{aligned} \quad (\text{S39})$$

For any $|\mathbf{u}_r^{\mathbf{X}'}\rangle \notin S_1^{(2)}$,

$$|\langle \chi_1^{(2)} | \mathbf{u}_r^{\mathbf{X}'} \rangle| = \mathcal{C}_1^{(2)} |\langle \chi_1^{(1)} | \mathbf{u}_r^{\mathbf{X}'} \rangle| \geq \frac{7}{8} \frac{1}{14R\sqrt{R}} = \frac{1}{16R\sqrt{R}}. \quad (\text{S40})$$

Therefore, $|\chi_1^{(2)}\rangle$ defined here can be employed as $|\chi_1\rangle$ that satisfies $1/\zeta_1 = O(\text{poly } R)$.

Likewise, a reference state $|\chi_2\rangle$ that satisfies $1/\zeta_2 = O(\text{poly } R)$ can be defined as

$$|\chi_2\rangle := \mathcal{C}_2^{(1)} \left[|\chi_2^{(0)}\rangle + \frac{1}{2\sqrt{R}} |\phi_2^{(1)}\rangle \right], \quad (\text{S41})$$

where $\mathcal{C}_2^{(1)}$ is the normalizing constant,

$$|\chi_2^{(0)}\rangle := \frac{1}{\sqrt{R}} \sum_{r=1}^R |\mathbf{v}_r^{\mathbf{X}^*}\rangle, \quad (\text{S42})$$

$$|\phi_2^{(1)}\rangle := \frac{1}{\sqrt{|S_2^{(1)}|}} \sum_{|\mathbf{v}_r^{\mathbf{X}'^*}\rangle \in S_2^{(1)}} |\mathbf{v}_r^{\mathbf{X}'^*}\rangle, \quad (\text{S43})$$

and

$$S_2^{(1)} := \left\{ |\mathbf{v}_r^{\mathbf{X}'^*}\rangle \mid r \in \{1, 2, \dots, R\}, |\langle \chi_2^{(0)} | \mathbf{v}_r^{\mathbf{X}'^*}\rangle| \leq \frac{1}{4R} \right\}. \quad (\text{S44})$$

Note that the qDMD algorithm does not need to estimate $\langle \chi_2 | \mathbf{v}_r^{[\mathbf{X} \ \mathbf{X}'^*]}\rangle$. Consequently, the above definition of $|\chi_2\rangle$ does not contain $|\mathbf{v}_r^{[\mathbf{X} \ \mathbf{X}'^*]}\rangle$.

B. Computation of $|\chi_1\rangle$ and $|\chi_2\rangle$: An example

We present quantum circuits that generate $|\chi_1\rangle$ and $|\chi_2\rangle$ defined in the previous subsection.

Initially, we perform pure-state tomography [3] to estimate all right singular vector states of \mathbf{X} , \mathbf{X}' , and $[\mathbf{X} \ \mathbf{X}']$. The pure-state tomography requires an $O(M)$ runtime for each right singular vector state of M dimensions. Subsequently, for each right singular vector state $|\mathbf{v}^*\rangle$, we construct a quantum circuit $U_{\mathbf{v}^*}$ such that $U_{\mathbf{v}^*} |0\rangle = |\mathbf{v}^*\rangle$ ¹. When the classical data of the amplitudes of $|\mathbf{v}^*\rangle$ is given, such a quantum circuit can be implemented with a gate complexity of $O(\text{poly log } M)$ [4, 5].

Next, we compute $|\chi_1^{(0)}\rangle$ with the following steps: (1) Prepare $|\text{SVD}([\mathbf{X} \ \hat{\mathbf{X}}']\rangle\rangle$. (2) Uncompute the second to fourth registers of $|\text{SVD}([\mathbf{X} \ \hat{\mathbf{X}}']\rangle\rangle$ by controlled- $U_{\mathbf{v}_r^{[\mathbf{X} \ \mathbf{X}'^*]}}^\dagger$ operations:

$$\begin{aligned} |\text{SVD}([\mathbf{X} \ \hat{\mathbf{X}}']\rangle\rangle &= \sum_{r=1}^R \hat{\sigma}_r^{[\mathbf{X} \ \mathbf{X}']} |\mathbf{u}_r^{[\mathbf{X} \ \mathbf{X}']}\rangle_1 |\mathbf{v}_r^{[\mathbf{X} \ \mathbf{X}'^*]}\rangle_{234} |(\hat{\sigma}_r^{[\mathbf{X} \ \mathbf{X}']})^2\rangle_5 \\ &\mapsto \sum_{r=1}^R \hat{\sigma}_r^{[\mathbf{X} \ \mathbf{X}']} |\mathbf{u}_r^{[\mathbf{X} \ \mathbf{X}']}\rangle_1 U_{\mathbf{v}_r^{[\mathbf{X} \ \mathbf{X}'^*]}}^\dagger |\mathbf{v}_r^{[\mathbf{X} \ \mathbf{X}'^*]}\rangle_{234} |(\hat{\sigma}_r^{[\mathbf{X} \ \mathbf{X}']})^2\rangle_5 \\ &= \sum_{r=1}^R \hat{\sigma}_r^{[\mathbf{X} \ \mathbf{X}']} |\mathbf{u}_r^{[\mathbf{X} \ \mathbf{X}']}\rangle_1 |0\rangle_{234} |(\hat{\sigma}_r^{[\mathbf{X} \ \mathbf{X}']})^2\rangle_5. \end{aligned} \quad (\text{S45})$$

Here, each $U_{\mathbf{v}_r^{[\mathbf{X} \ \mathbf{X}'^*]}}^\dagger$ is applied to the second to fourth registers of $|\text{SVD}([\mathbf{X} \ \hat{\mathbf{X}}']\rangle\rangle$ conditionally on the fifth register. (3) Add an ancilla qubit (the sixth register). (4) Compute the following state by controlled rotations of the ancilla qubit conditionally on the fifth register:

$$\sum_{r=1}^R \hat{\sigma}_r^{[\mathbf{X} \ \mathbf{X}']} |\mathbf{u}_r^{[\mathbf{X} \ \mathbf{X}']}\rangle_1 |0\rangle_{234} |(\hat{\sigma}_r^{[\mathbf{X} \ \mathbf{X}']})^2\rangle_5 \left[\frac{a_0}{\hat{\sigma}_r^{[\mathbf{X} \ \mathbf{X}']}\sqrt{R}} |0\rangle_6 + \sqrt{1 - \left| \frac{a_0}{\hat{\sigma}_r^{[\mathbf{X} \ \mathbf{X}']}\sqrt{R}} \right|^2} |1\rangle_6 \right], \quad (\text{S46})$$

¹ Because the pure-state tomography can not determine the global phase of a right singular vector state, the unitary gate $U_{\mathbf{v}^*}$ may act as $U_{\mathbf{v}^*} |0\rangle = \exp(-i\varphi) |\mathbf{v}^*\rangle$ where φ signifies the unknown global phase. This unknown phase factor will change the relative phase of the associated left and right singular vector states in the computed reference states. However, such phase factor does not violate the condition $1/\zeta = O(\text{poly } R)$ proven in the previous subsection. Thus, we omit the phase factor for simplicity in this section.

where a_0 is a constant such that

$$\frac{a_0}{\hat{\sigma}_r^{[\mathbf{X} \ \mathbf{X}']} \sqrt{R}} \leq 1, \quad \forall r \in \{1, 2, \dots, R\}. \quad (\text{S47})$$

This condition is the necessary and sufficient condition for the controlled rotations to be possible and is equivalent to

$$a_0 \leq \sqrt{R} \min_r \hat{\sigma}_r^{[\mathbf{X} \ \mathbf{X}']}. \quad (\text{S48})$$

(5) Uncompute the fifth register by the inverse transform of the quantum SVD process. Specifically, the inverse process consists of the inverse quantum Fourier transform of the fifth register and the density matrix exponentiation multiplying $\exp(-i \text{tr}_{234}(|[\mathbf{X} \ \hat{\mathbf{X}}']\rangle\langle[\mathbf{X} \ \hat{\mathbf{X}}']|)t)$ to the first register conditioned on the fifth register. Here, tr_{234} denotes the partial trace with respect to the second to fourth registers. See [6] for the details of the quantum SVD process. (6) Measure the second to sixth registers. If all measured values are zero, we obtain $|\chi_1^{(0)}\rangle_1 |0\rangle_{2:6}$. The success probability is a_0^2 . When $\sqrt{R} \min_r \hat{\sigma}_r^{[\mathbf{X} \ \mathbf{X}]}$ is employed as a_0 , an asymptotic lower bound of the success probability can be evaluated as

$$a_0^2 = R(\min_r \hat{\sigma}_r^{[\mathbf{X} \ \mathbf{X}']})^2 = \Omega\left(R \frac{1}{R\kappa_{[\mathbf{X} \ \mathbf{X}']}^2}\right) = \Omega\left(\frac{1}{\kappa^2}\right). \quad (\text{S49})$$

Here, $\kappa_{\mathbf{Z}}$ denotes the condition number of \mathbf{Z} ($\mathbf{Z} = \mathbf{X}, \mathbf{X}', [\mathbf{X} \ \mathbf{X}']$) defined in Eq. (S8), $\kappa := \max_{\mathbf{Z}} \kappa_{\mathbf{Z}}$, and we use Eq. (S16) to derive the lower bound. In summary, we can compute $|\chi_1^{(0)}\rangle$ by $O(\kappa^2 R)$ controlled- $U_{\psi^*}^\dagger$ operations and $O(\kappa^2)$ forward and inverse quantum SVD operations.

Having established the computation for $|\chi_1^{(0)}\rangle$, we next address the computation for $|\chi_1^{(1)}\rangle$: (1) Determine whether each $|\mathbf{u}_r^{\mathbf{X}}\rangle$ belongs to $S_1^{(1)}$ using the two-state SWAP test between $|\chi_1^{(0)}\rangle$ and $|\mathbf{u}_r^{\mathbf{X}}\rangle$. If $|S_1^{(1)}| = 0$, then $|\chi_1^{(1)}\rangle = |\chi_1^{(0)}\rangle$. Thus we consider the case that $|S_1^{(1)}| \geq 1$ below. (2) Prepare the following state:

$$|[\mathbf{X} \ \hat{\mathbf{X}}']\rangle_{1:4} |0\rangle_5 |0\rangle_6 \left[\frac{1}{\sqrt{2}} (|0\rangle_7 + |1\rangle_7) \right], \quad (\text{S50})$$

where the fifth register is an ancilla register for indicating singular values, and the sixth and seventh registers are one-qubit ancilla registers. Note that $|[\mathbf{X} \ \hat{\mathbf{X}}']\rangle_{1:4}$ can be written as

$$|[\mathbf{X} \ \hat{\mathbf{X}}']\rangle_{1:4} = \sqrt{P_{\mathbf{X}}} |\hat{\mathbf{X}}\rangle_{123} |0\rangle_4 + \sqrt{P_{\mathbf{X}'}} |\hat{\mathbf{X}}'\rangle_{123} |1\rangle_4, \quad (\text{S51})$$

with

$$P_{\mathbf{Z}} = \frac{\|\mathbf{Z}\|_{\mathbb{F}}^2}{\|[\mathbf{X} \ \mathbf{X}']\|_{\mathbb{F}}^2}, \quad \mathbf{Z} \in \{\mathbf{X}, \mathbf{X}'\}. \quad (\text{S52})$$

Thus the prepared state is

$$\begin{aligned} & \frac{1}{\sqrt{2}} |[\mathbf{X} \ \hat{\mathbf{X}}']\rangle_{1:4} |0\rangle_5 |0\rangle_6 |0\rangle_7 \\ & + \frac{1}{\sqrt{2}} \left[\sqrt{P_{\mathbf{X}}} |\hat{\mathbf{X}}\rangle_{123} |0\rangle_4 |0\rangle_5 |0\rangle_6 |1\rangle_7 + \sqrt{P_{\mathbf{X}'}} |\hat{\mathbf{X}}'\rangle_{123} |1\rangle_4 |0\rangle_5 |0\rangle_6 |1\rangle_7 \right]. \end{aligned} \quad (\text{S53})$$

(3) Perform the steps 1–5 of computing $|\chi_1^{(0)}\rangle$ described above conditionally on the seventh register to get

$$\frac{1}{\sqrt{2}} a_0 |\chi_1^{(0)}\rangle_1 |0\rangle_{2:6} |0\rangle_7 + \frac{1}{\sqrt{2}} \sqrt{P_{\mathbf{X}}} |\hat{\mathbf{X}}\rangle_{123} |0\rangle_4 |0\rangle_5 |0\rangle_6 |1\rangle_7 + \dots \quad (\text{S54})$$

In the computation for $|\chi_1^{(1)}\rangle$, the constant a_0 is specified as

$$a_0 = \min \left\{ \sqrt{R} \min_r \hat{\sigma}_r^{[\mathbf{X} \ \mathbf{X}']}, 2\sqrt{P_{\mathbf{X}} R |S_1^{(1)}|} \min_{r \in \text{ind } S_1^{(1)}} \hat{\sigma}_r^{\mathbf{X}} \right\}, \quad (\text{S55})$$

where

$$\text{ind } S_1^{(1)} := \left\{ r \in \{1, 2, \dots, R\} \mid |\mathbf{u}_r^{\mathbf{X}}\rangle \in S_1^{(1)} \right\}. \quad (\text{S56})$$

The reason of this specific choice is clarified in the next step. (4) In a similar way to computing $|\chi_1^{(0)}\rangle$, compute $|\phi_1^{(1)}\rangle$ conditionally on the fourth and seventh register:

$$\frac{1}{\sqrt{2}} a_0 |\chi_1^{(0)}\rangle_1 |0\rangle_{2:6} |0\rangle_7 + \frac{1}{\sqrt{2}} \sqrt{P_{\mathbf{X}}} a_1 |\phi_1^{(1)}\rangle_1 |0\rangle_{2:6} |1\rangle_7 + \dots \quad (\text{S57})$$

Here, a_1 is a constant related to controlled-rotations and needs to satisfy

$$a_1 \leq \sqrt{|S_1^{(1)}|} \min_{r \in \text{ind } S_1^{(1)}} \hat{\sigma}_r^{\mathbf{X}}. \quad (\text{S58})$$

In the present computation, we choose a_1 as

$$a_1 = \frac{a_0}{2\sqrt{P_{\mathbf{X}}R}}. \quad (\text{S59})$$

This choice is possible owing to the aforementioned choice of a_0 . Consequently, we have the following state:

$$\frac{1}{\sqrt{2}} a_0 \left[|\chi_1^{(0)}\rangle_1 |0\rangle_{2:6} |0\rangle_7 + \frac{1}{2\sqrt{R}} |\phi_1^{(1)}\rangle_1 |0\rangle_{2:6} |1\rangle_7 \right] + \dots \quad (\text{S60})$$

(5) Apply the Hadamard gate to the seventh register to get

$$\frac{1}{2} a_0 \left[|\chi_1^{(0)}\rangle_1 + \frac{1}{2\sqrt{R}} |\phi_1^{(1)}\rangle_1 \right] |0\rangle_{2:7} + \dots \quad (\text{S61})$$

(6) Measure the second to seventh registers. If all measured values are zero, we obtain $|\chi_1^{(1)}\rangle_1 |0\rangle_{2:7}$. The success probability is $(a_0/2\mathcal{C}_1^{(1)})^2$. A lower bound of this probability can be evaluated as

$$\begin{aligned} \left(\frac{a_0}{2\mathcal{C}_1^{(1)}} \right)^2 &\geq \frac{P_{\mathbf{X}}R \min_{\mathbf{Z}} \min_r (\hat{\sigma}_r^{\mathbf{Z}})^2}{4} \left[\|\chi_1^{(0)}\| - \frac{1}{2\sqrt{R}} \|\phi_1^{(1)}\| \right]^2 \\ &= \Omega \left(\frac{1}{\eta\kappa^2} \right). \end{aligned} \quad (\text{S62})$$

Therefore, we can compute $|\chi_1^{(1)}\rangle$ by $O(\eta\kappa^2R)$ controlled- U_{*}^{\dagger} operations and $O(\eta\kappa^2)$ forward and inverse quantum SVD operations.

The reference state $|\chi_1\rangle$ now can be computed as follows: (1) In a similar way of computing $|\chi_1^{(1)}\rangle$, compute

$$\begin{aligned} &\frac{1}{\sqrt{2}} a_0 |\chi_1^{(0)}\rangle_1 |0\rangle_{23} |0\rangle_4 |0\rangle_5 |0\rangle_6 |0\rangle_7 \\ &+ \frac{1}{\sqrt{2}} \sqrt{P_{\mathbf{X}}} a_1 |\phi_1^{(1)}\rangle_1 |0\rangle_{23} |0\rangle_4 |0\rangle_5 |0\rangle_6 |1\rangle_7 \\ &+ \frac{1}{\sqrt{2}} \sqrt{P_{\mathbf{X}'}} a_2 |\phi_1^{(2)}\rangle_1 |0\rangle_{23} |1\rangle_4 |0\rangle_5 |0\rangle_6 |1\rangle_7 + \dots \end{aligned} \quad (\text{S63})$$

Here, we define the constants a_0 , a_1 , and a_2 as

$$a_0 = \min \left\{ \sqrt{R} \min_r \hat{\sigma}_r^{[\mathbf{X} \ \mathbf{X}']}, \sqrt{2P_{\mathbf{X}}R} |S_1^{(1)}| \min_{r \in \text{ind } S_1^{(1)}} \hat{\sigma}_r^{\mathbf{X}}, \sqrt{\frac{(7\mathcal{C}_1^{(1)})^2 P_{\mathbf{X}'} R^2 |S_1^{(2)}|}{2}} \min_{r \in \text{ind } S_1^{(2)}} \hat{\sigma}_r^{\mathbf{X}'} \right\}, \quad (\text{S64})$$

$$a_1 = a_0 \sqrt{\frac{1}{2P_{\mathbf{X}}R}}, \quad (\text{S65})$$

$$a_2 = a_0 \sqrt{\frac{2}{(7\mathcal{C}_1^{(1)})^2 P_{\mathbf{X}'} R^2}}, \quad (\text{S66})$$

where

$$\text{ind } S_1^{(2)} := \left\{ r \in \{1, 2, \dots, R\} \mid |\mathbf{u}_r^{\mathbf{X}'}\rangle \in S_1^{(2)} \right\}. \quad (\text{S67})$$

Note that $S_1^{(2)}$ can be determined by the two-state SWAP test between $|\chi_1^{(1)}\rangle$ and $|\mathbf{u}_r^{\mathbf{X}'}\rangle$ and that the value of $\mathcal{C}_1^{(1)}$ can be estimated through the success probability of computing $|\chi_1^{(1)}\rangle$. Consequently, we have the following state:

$$\begin{aligned} & \frac{a_0}{\sqrt{2}} |\chi_1^{(0)}\rangle_1 |0\rangle_{2:6} |0\rangle_7 \\ & + a_0 \left[\frac{1}{2\sqrt{R}} |\phi_1^{(1)}\rangle_1 |0\rangle_{23} |0\rangle_4 |0\rangle_{56} |1\rangle_7 + \frac{1}{7\mathcal{C}_1^{(1)}R} |\phi_1^{(2)}\rangle_1 |0\rangle_{23} |1\rangle_4 |0\rangle_{56} |1\rangle_7 \right] + \dots \end{aligned} \quad (\text{S68})$$

(2) Apply the Hadamard gate to the fourth register conditionally on the seventh register to get

$$\frac{a_0}{\sqrt{2}} \left[|\chi_1^{(0)}\rangle_1 |0\rangle_{2:6} |0\rangle_7 + \frac{1}{2\sqrt{R}} |\phi_1^{(1)}\rangle_1 |0\rangle_{2:6} |1\rangle_7 + \frac{1}{7\mathcal{C}_1^{(1)}R} |\phi_1^{(2)}\rangle_1 |0\rangle_{2:6} |1\rangle_7 \right] + \dots \quad (\text{S69})$$

(3) Apply the Hadamard gate to the seventh register to get

$$\frac{a_0}{2\mathcal{C}_1^{(1)}} \left[\mathcal{C}_1^{(1)} \left(|\chi_1^{(0)}\rangle_1 + \frac{1}{2\sqrt{R}} |\phi_1^{(1)}\rangle_1 \right) + \frac{1}{7R} |\phi_1^{(2)}\rangle_1 \right] |0\rangle_{2:7} + \dots \quad (\text{S70})$$

(4) Measure the second to seventh registers. If all measured values are zero, we obtain $|\chi_1\rangle_1 |0\rangle_{2:7}$. The success probability is $(a_0/\mathcal{C}_1^{(2)}\mathcal{C}_1^{(1)})^2$, which is $\Omega(1/\eta\kappa^2)$. Therefore, we can compute $|\chi_1\rangle$ by $O(\eta\kappa^2R)$ controlled- $U_{\mathbf{v}^*}^\dagger$ operations and $O(\eta\kappa^2)$ forward and inverse quantum SVD operations.

Next, let us consider how to generate $|\chi_2^{(0)}\rangle$: (1) Prepare the following state:

$$\frac{1}{\sqrt{R}} \sum_{r=1}^R |0\rangle_{23} |(\hat{\sigma}_r^{\mathbf{X}})^2\rangle_5. \quad (\text{S71})$$

(2) Apply $U_{\mathbf{v}_r^{\mathbf{X}^*}}$ conditionally on the fifth register to get:

$$\frac{1}{\sqrt{R}} \sum_{r=1}^R U_{\mathbf{v}_r^{\mathbf{X}^*}} |0\rangle_{23} |(\hat{\sigma}_r^{\mathbf{X}})^2\rangle_5 = \frac{1}{\sqrt{R}} \sum_{r=1}^R |\mathbf{v}_r^{\mathbf{X}^*}\rangle_{23} |(\hat{\sigma}_r^{\mathbf{X}})^2\rangle_5. \quad (\text{S72})$$

(3) Uncompute the fifth register by the inverse quantum SVD:

$$\frac{1}{\sqrt{R}} \sum_{r=1}^R |\mathbf{v}_r^{\mathbf{X}^*}\rangle_{23} |0\rangle_5. \quad (\text{S73})$$

Here, the inverse quantum SVD consists of the inverse quantum Fourier transform of the fifth register and the density matrix exponentiation multiplying $\exp(-i \text{tr}_1(|\hat{\mathbf{X}}\rangle\langle\hat{\mathbf{X}}|)t)$ to the second and third register conditioned on the fifth register. The symbol tr_1 signifies the partial trace with respect to the first register. Thus we can compute $|\chi_2^{(0)}\rangle$ by R controlled- $U_{\mathbf{v}^*}$ operations and one inverse quantum SVD operation.

Lastly, we present the computation of $|\chi_2\rangle$: (1) Prepare the following state:

$$\sqrt{\frac{1}{1 + \frac{1}{4R}}} \left[\frac{1}{\sqrt{R}} \sum_{r=1}^R |0\rangle_{23} |0\rangle_4 |(\hat{\sigma}_r^{\mathbf{X}})^2\rangle_5 + \frac{1}{2\sqrt{R|S_2^{(1)}|}} \sum_{r \in \text{ind } S_2^{(1)}} |0\rangle_{23} |1\rangle_4 |(\hat{\sigma}_r^{\mathbf{X}'})^2\rangle_5 \right], \quad (\text{S74})$$

where

$$\text{ind } S_2^{(1)} := \left\{ r \in \{1, 2, \dots, R\} \mid |\mathbf{v}_r^{\mathbf{X}'^*}\rangle \in S_2^{(1)} \right\}. \quad (\text{S75})$$

(2) Compute $|\chi_2^{(0)}\rangle$ and $|\phi_2^{(1)}\rangle$ conditionally on the fourth register in a similar way to the steps 2 and 3 of computing $|\chi_2^{(0)}\rangle$ described above:

$$\sqrt{\frac{1}{1 + \frac{1}{4R}}} \left[\frac{1}{\sqrt{R}} \sum_{r=1}^R |\mathbf{v}_r^{\mathbf{X}^*}\rangle_{23} |0\rangle_4 |0\rangle_5 + \frac{1}{2\sqrt{R|S_2^{(1)}|}} \sum_{r \in \text{ind } S_2^{(1)}} |\mathbf{v}_r^{\mathbf{X}'^*}\rangle_{23} |1\rangle_4 |0\rangle_5 \right]. \quad (\text{S76})$$

(3) Apply the Hadamard gate to the fourth register. Then we have

$$\frac{1}{\sqrt{2}} \sqrt{\frac{1}{1 + \frac{1}{4R}}} \left[\frac{1}{\sqrt{R}} \sum_{r=1}^R |\mathbf{v}_r^{\mathbf{X}^*}\rangle_{23} + \frac{1}{2\sqrt{R|S_2^{(1)}|}} \sum_{r \in \text{ind } S_2^{(1)}} |\mathbf{v}_r^{\mathbf{X}'^*}\rangle_{23} \right] |0\rangle_{45} + \dots \quad (\text{S77})$$

(4) Measure the fourth and fifth registers. If the outcome corresponds to all zeros, we obtain $|\chi_2\rangle_{23}|0\rangle_{45}$. The success probability is $1/[(2 + 1/2R)(C_2^{(1)})^2]$, which is $\Omega(1)$. Therefore we can compute $|\chi_2\rangle$ by $O(R)$ controlled- $U_{\mathbf{v}^*}$ operations and $O(1)$ inverse quantum SVD operations.

The presented quantum processes that compute $|\chi_1\rangle$ and $|\chi_2\rangle$ are not unitary because they include post selection steps. Instead, they are block encodings of the unitary gates U_{χ_1} and U_{χ_2} . Even in this case, it is still possible to perform the inner product estimation presented in the main text. However, the computational complexity increases according to the success probability of the post selection. Specifically, it increases by a factor of $O(\eta\kappa^2)$ in the present case.

C. Summary and concluding remarks

The example of the reference state preparation presented in this section demonstrates the existence of quantum circuits with polylogarithmic complexity in terms of N , capable of generating $|\chi_1\rangle$ and $|\chi_2\rangle$ such that $1/\zeta = O(\text{poly } R)$. The construction of these circuits necessitates the pure-state tomography of right singular vector states. Consequently, the computational complexity of constructing the presented circuits increases linearly with M , while the execution of the presented circuits is much more efficient with $O(\text{poly log } M)$ complexity.

It is important to note that while this example serves as a theoretical construct to demonstrate that the qDMD algorithm can achieve an exponential speedup in N , it is not optimized for practical use. For specific problems, one may find more efficient ways to prepare reference states. For instance, methods like the automatic quantum circuit encoding [7] may construct quantum circuits that approximately generate singular vector states or their superpositions without exhaustive tomography. Furthermore, the value of ζ may be enhanced in a variational manner in which a parameterized ansatz quantum circuit is tuned based on observed inner product values. Such variational method may improve the scaling of the computational complexity relative to R . The development of a pragmatic approach to the reference state preparation remains an open area for future research.

III. COMPUTING DMD MODE STATES

A. Recursive coherent state addition

The quantum circuit proposed by Oszmaniec et al. [8] (Fig. 3 of the main text) creates a coherent superposition of two quantum states $|\psi_0\rangle$ and $|\psi_1\rangle$:

$$|\Psi\rangle = \alpha \frac{\langle\chi|\psi_1\rangle}{|\langle\chi|\psi_1\rangle|} |\psi_0\rangle + \beta \frac{\langle\chi|\psi_0\rangle}{|\langle\chi|\psi_0\rangle|} |\psi_1\rangle. \quad (\text{S78})$$

Here, α and β are user-specified complex amplitudes, and $|\chi\rangle$ is a reference quantum state for the coherent addition. When $|\psi_0\rangle$ and $|\psi_1\rangle$ are orthogonal—the computation of DMD mode states satisfies this condition—the probability of successfully creating the coherent superposition is given by

$$\frac{|\langle\chi|\psi_0\rangle|^2 |\langle\chi|\psi_1\rangle|^2}{|\langle\chi|\psi_0\rangle|^2 + |\langle\chi|\psi_1\rangle|^2}. \quad (\text{S79})$$

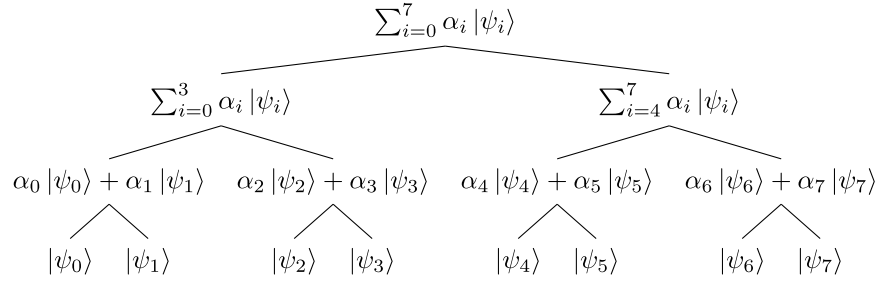


FIG. S1. Recursive coherent state addition for creating a superposition of multiple quantum states. This figure illustrates the case for an eight-state superposition. The root node represents the target superposition of multiple quantum states. The leaf nodes correspond to elementary quantum states comprising the target superposition. Each branch node (a non-leaf node) represents a coherent superposition of its child nodes, up to normalization. The process advances from the bottom to the top, where the superposition at each branch node is created from the coherent addition of its child nodes.

The created superposition can also be represented as

$$\begin{aligned} |\Psi\rangle &= \alpha e^{i\theta_1} |\psi_0\rangle + \beta e^{i\theta_0} |\psi_1\rangle \\ &= e^{i(\theta_0+\theta_1)} [\alpha e^{-i\theta_0} |\psi_0\rangle + \beta e^{-i\theta_1} |\psi_1\rangle], \end{aligned} \quad (\text{S80})$$

where

$$\theta_i = \arg \langle \chi | \psi_i \rangle \quad (\text{S81})$$

for $i = 0, 1$. If the global phase of $|\psi_i\rangle$ is shifted by θ , the phase θ_i is also shifted by θ . Therefore, the phase factor $\exp(-i\theta_i)$ of the amplitude of $|\psi_i\rangle$ ensures that the superposition state $|\Psi\rangle$ is invariant up to its global phase under a global phase shift of $|\psi_i\rangle$. When θ_0 and θ_1 are known, including the phase factors $\exp(i\theta_0)$ and $\exp(i\theta_1)$ into user-specified amplitudes α and β , one can create a superposition of two quantum states with arbitrary amplitudes.

One can also create a coherent superposition of multiple quantum states by recursively creating two-state coherent superpositions. This recursive coherent state addition process is illustrated in Fig. S1. In this figure, the multi-state coherent addition process proceeds from the bottom to the top; the superposition state at each branch node is created by the two-state coherent addition of its child nodes' states. One may adopt different reference states for each two-state coherent addition process to enhance the success probability of each process (see below).

The recursive coherent state addition protocol allows for the computation of a DMD mode state. Suppose we aim to compute a DMD mode state

$$|\tilde{w}_r\rangle \approx \sum_{r'=1}^R \tilde{w}_r^{r'} |\mathbf{u}_{r'}^{[\mathbf{X} \ \mathbf{X}']}\rangle. \quad (\text{S82})$$

The recursive coherent state addition consists of $R-1$ steps of two-state coherent addition in this case. Let us consider a two-state coherent addition step indexed by k that adds two quantum states

$$|\psi_{I_0^k}\rangle = \frac{1}{\sqrt{\sum_{r' \in I_0^k} |\tilde{w}_r^{r'}|^2}} \sum_{r' \in I_0^k} \tilde{w}_r^{r'} |\mathbf{u}_{r'}^{[\mathbf{X} \ \mathbf{X}']}\rangle, \quad (\text{S83})$$

$$|\psi_{I_1^k}\rangle = \frac{1}{\sqrt{\sum_{r' \in I_1^k} |\tilde{w}_r^{r'}|^2}} \sum_{r' \in I_1^k} \tilde{w}_r^{r'} |\mathbf{u}_{r'}^{[\mathbf{X} \ \mathbf{X}']}\rangle, \quad (\text{S84})$$

to create the superposition state

$$|\psi_{I_0^k \cup I_1^k}\rangle = \frac{1}{\sqrt{\sum_{r' \in I_0^k \cup I_1^k} |\tilde{w}_r^{r'}|^2}} \sum_{r' \in I_0^k \cup I_1^k} \tilde{w}_r^{r'} |\mathbf{u}_{r'}^{[\mathbf{X} \ \mathbf{X}']}\rangle. \quad (\text{S85})$$

Here, I_0^k and I_1^k are some mutually-exclusive sets of indices r' . The user-specified amplitude of $|\psi_{I_j^k}\rangle$ ($j = 0, 1$) to create $|\psi_{I_0^k \cup I_1^k}\rangle$ is given by

$$\sqrt{\frac{\sum_{r' \in I_j^k} |\tilde{w}_r^{r'}|^2}{\sum_{r' \in I_0^k \cup I_1^k} |\tilde{w}_r^{r'}|^2}} e^{i\theta_{I_j^k}}, \quad (\text{S86})$$

where

$$\theta_{I_j^k} = \arg \langle \chi_{\text{add}}^k | \psi_{I_j^k} \rangle, \quad (\text{S87})$$

and $|\chi_{\text{add}}^k\rangle$ denotes the reference state for the two-state coherent addition of step k . The inner product $\langle \chi_{\text{add}}^k | \psi_{I_j^k} \rangle$ can be calculated through the equation

$$\langle \chi_{\text{add}}^k | \psi_{I_j^k} \rangle = \frac{1}{\sqrt{\sum_{r' \in I_j^k} |\tilde{w}_{r'}^{r'}|^2}} \sum_{r' \in I_j^k} \tilde{w}_{r'}^{r'} \langle \chi_{\text{add}}^k | \mathbf{u}_{r'}^{[\mathbf{X} \ \mathbf{X}']} \rangle \quad (\text{S88})$$

and the estimation of $\{\langle \chi_{\text{add}}^k | \mathbf{u}_{r'}^{[\mathbf{X} \ \mathbf{X}']} \rangle\}$. To estimate $\langle \chi_{\text{add}}^k | \mathbf{u}_{r'}^{[\mathbf{X} \ \mathbf{X}']} \rangle$, we perform the three-state SWAP test for $|\chi_{\text{add}}^k\rangle$, $|\mathbf{u}_{r'}^{[\mathbf{X} \ \mathbf{X}']}\rangle$, and $|\chi_1\rangle$, which provides an estimate of $\langle \chi_{\text{add}}^k | \mathbf{u}_{r'}^{[\mathbf{X} \ \mathbf{X}']} \rangle \langle \mathbf{u}_{r'}^{[\mathbf{X} \ \mathbf{X}']} | \chi_1 \rangle \langle \chi_1 | \chi_{\text{add}}^k \rangle$. The inner product $\langle \mathbf{u}_{r'}^{[\mathbf{X} \ \mathbf{X}']} | \chi_1 \rangle$ is known through the estimation of $\tilde{\mathbf{K}}'$. The inner product $\langle \chi_1 | \chi_{\text{add}}^k \rangle$ can be estimated as follows. Recall that the reference states $|\chi_1\rangle$ and $|\chi_{\text{add}}^k\rangle$ are assumed to be prepared unitary gates U_{χ_1} and $U_{\chi_{\text{add}}^k}$, respectively². Using these unitary gates conditionally, we compute the following state:

$$\frac{U_{\chi_1} |0\rangle_1 |0\rangle_a + U_{\chi_{\text{add}}^k} |0\rangle_1 |1\rangle_a}{\sqrt{2}} = \frac{|\chi_1\rangle_1 |0\rangle_a + |\chi_{\text{add}}^k\rangle_1 |1\rangle_a}{\sqrt{2}}, \quad (\text{S89})$$

where $| \rangle_a$ denotes a ket of an ancilla control qubit. When the above state is input to the circuit depicted in Fig. 2 of the main text, the circuit provides an estimate of $\langle \chi_1 | \chi_{\text{add}}^k \rangle$. Therefore, we can estimate the inner products $\{\langle \chi_{\text{add}}^k | \mathbf{u}_{r'}^{[\mathbf{X} \ \mathbf{X}']} \rangle\}$ and calculate $\langle \chi_{\text{add}}^k | \psi_{I_j^k} \rangle$. In this way, we determine the user-specified amplitudes in each step k . By repeating two-state coherent addition processes recursively in the manner shown in Fig. S1, we get the desired DMD mode vector state.

B. Computational complexity

Let us evaluate the computational complexity of computing a DMD mode state with keeping the phase error of each amplitude $\tilde{w}_{r'}^{r'}$ below ϵ . The computational complexity consists of two contributing parts: (1) the computational complexity of estimating phases $\theta_{I_0^k}$ and $\theta_{I_1^k}$ at all steps k and (2) the computational complexity of the recursive coherent state addition. In the following evaluation, we omit the computational costs for reference state preparations, which will be considered in the next subsection.

First, we consider the computational complexity of estimating phases $\theta_{I_0^k}$ and $\theta_{I_1^k}$ at all steps k . Because the tree depth for the recursive coherent state addition is $\lceil \log_2 R \rceil$, the tolerant phase error at each step is $\epsilon / \lceil \log_2 R \rceil$. Therefore, at each step k , it is necessary to estimate $\langle \chi_{\text{add}}^k | \psi_{I_j^k} \rangle$ with precision³

$$\frac{2}{\pi} |\langle \chi_{\text{add}}^k | \psi_{I_j^k} \rangle| \frac{\epsilon}{\lceil \log_2 R \rceil}. \quad (\text{S90})$$

The estimation error of $\langle \chi_{\text{add}}^k | \psi_{I_j^k} \rangle$ is bounded from above by the sum of the estimation errors of the terms on the right hand side of Eq. (S88). Let ϵ_{term} denote the maximum error of $\{\langle \chi_{\text{add}}^k | \mathbf{u}_{r'}^{[\mathbf{X} \ \mathbf{X}']} \rangle\}$. Then, the estimation error of $\langle \chi_{\text{add}}^k | \psi_{I_j^k} \rangle$ is bounded from above by

$$\frac{\sum_{r' \in I_j^k} |\tilde{w}_{r'}^{r'}|}{\sqrt{\sum_{r' \in I_j^k} |\tilde{w}_{r'}^{r'}|^2}} \epsilon_{\text{term}} \leq \sqrt{|I_j^k|} \epsilon_{\text{term}} \leq \sqrt{R} \epsilon_{\text{term}}. \quad (\text{S91})$$

The first inequality follows the Cauchy–Schwarz inequality. Consequently,

$$\epsilon_{\text{term}} = \frac{2}{\pi} |\langle \chi_{\text{add}}^k | \psi_{I_j^k} \rangle| \frac{\epsilon}{\sqrt{R} \lceil \log_2 R \rceil} \quad (\text{S92})$$

² Instead of the assumption of the unitarity of the reference state preparation, the assumption of the availability of block encodings of U_{χ_1} and $U_{\chi_{\text{add}}^k}$ also makes the argument in the present subsection valid, although the computational complexity may increase.

³ Let \tilde{z} be an estimate of a complex value z and ϵ_z denote the estimation error, i.e., $\tilde{z} = z + \epsilon_z$. Here, we assume that $|\epsilon_z| < |z|$. On the complex plane, when the absolute value of ϵ_z is fixed, \tilde{z} lies on the circle centered at z with radius $|\epsilon_z|$. The phase error $\epsilon_{\text{phase}} = |\arg \tilde{z} - \arg z|$ takes the maximum when the line passing through \tilde{z} and the origin is tangent to the circle. The maximum value of ϵ_{phase} is $\arcsin(|\epsilon_z/z|)$. Because $\arcsin(|\epsilon_z/z|)$ is less than $(\pi/2)|\epsilon_z/z|$, the estimation of z with precision $(2/\pi)|z|\epsilon$ ensures that the phase error is less than ϵ .

is a sufficient condition for the desired total precision. This precision ϵ_{term} is achieved when $\langle \mathbf{u}_{r'}^{[\mathbf{X} \ \mathbf{X}']} | \chi_1 \rangle$, $\langle \chi_1 | \chi_{\text{add}}^k \rangle$, and $\langle \chi_{\text{add}}^k | \mathbf{u}_{r'}^{[\mathbf{X} \ \mathbf{X}']} \rangle \langle \mathbf{u}_{r'}^{[\mathbf{X} \ \mathbf{X}']} | \chi_1 \rangle \langle \chi_1 | \chi_{\text{add}}^k \rangle$ are estimated with precision of the order of

$$\frac{2}{\pi} |\langle \chi_{\text{add}}^k | \psi_{I_j^k} \rangle \langle \mathbf{u}_{r'}^{[\mathbf{X} \ \mathbf{X}']} | \chi_1 \rangle \langle \chi_1 | \chi_{\text{add}}^k \rangle| \frac{\epsilon}{\sqrt{R} \lceil \log_2 R \rceil}. \quad (\text{S93})$$

Let us define parameters ζ_3 and ζ_4 as

$$\zeta_3 := \min_k |\langle \chi_1 | \chi_{\text{add}}^k \rangle|^2, \quad (\text{S94})$$

$$\zeta_4 := \min_k \min_{j \in \{0,1\}} |\langle \chi_{\text{add}}^k | \psi_{I_j^k} \rangle|^2, \quad (\text{S95})$$

where \min_k signifies the minimum over all step-indices k . Additionally, ζ_1 defined in Eq. (S11) is a lower bound for $|\langle \mathbf{u}_{r'}^{[\mathbf{X} \ \mathbf{X}']} | \chi_1 \rangle|^2$. Using these parameters, we can express the required number of copies of each $|\mathbf{u}_{r'}^{[\mathbf{X} \ \mathbf{X}']}\rangle$ for estimating the phase factors at each step as $O(R(\log_2 R)^2 / \zeta_1 \zeta_3 \zeta_4 \epsilon^2)$. Because each $|\mathbf{u}_{r'}^{[\mathbf{X} \ \mathbf{X}']}\rangle$ is involved in $\lceil \log_2 R \rceil$ steps of two-state coherent addition, the required number of quantum SVDs for estimating all phase factors is

$$O\left(\frac{\kappa_{[\mathbf{X} \ \mathbf{X}']}^2}{\zeta_1 \zeta_3 \zeta_4 \epsilon^2} R^2 (\log_2 R)^3 \log(\kappa_{[\mathbf{X} \ \mathbf{X}']}^2 \log R)\right), \quad (\text{S96})$$

due to Eq. (S9). The parameter $\kappa_{[\mathbf{X} \ \mathbf{X}]}$ is the condition number of $[\mathbf{X} \ \mathbf{X}']$ (see Eq. (S8)). The gate complexity is larger than the required number of quantum SVDs by a factor of $T/\epsilon^2 \text{ poly log}(NM/\epsilon)$.

Next, we consider the computational complexity of the recursive coherent addition. The success probability at step k can be bounded from below as

$$\frac{|\langle \chi_{\text{add}}^k | \psi_{I_0^k} \rangle|^2 |\langle \chi_{\text{add}}^k | \psi_{I_1^k} \rangle|^2}{|\langle \chi_{\text{add}}^k | \psi_{I_0^k} \rangle|^2 + |\langle \chi_{\text{add}}^k | \psi_{I_1^k} \rangle|^2} \geq \frac{1}{2} \min\{|\langle \chi_{\text{add}}^k | \psi_{I_0^k} \rangle|^2, |\langle \chi_{\text{add}}^k | \psi_{I_1^k} \rangle|^2\} \geq \frac{\zeta_4}{2}. \quad (\text{S97})$$

Therefore, $O(2/\zeta_4)$ copies of $|\psi_{I_j^k}\rangle$ ($j = 0, 1$) are required for successfully creating a superposition state at step k . Because the tree depth for the recursive coherent state addition is $\lceil \log_2 R \rceil < \log_2 R + 1$, the required number of copies of $|\mathbf{u}_{r'}^{[\mathbf{X} \ \mathbf{X}']}\rangle$ is $O((2/\zeta_4)^{\log_2 R + 1})$ in total. Due to Eq. (S9), the required number of quantum SVDs for the recursive coherent state addition is

$$O\left(\frac{\kappa_{[\mathbf{X} \ \mathbf{X}']}^2}{\zeta_4} R^{2 + \log_2 \frac{1}{\zeta_4}} \log(\kappa_{[\mathbf{X} \ \mathbf{X}']}^2 \log R)\right). \quad (\text{S98})$$

The gate complexity is larger than the required number of quantum SVDs by a factor of $T/\epsilon^2 \text{ poly log}(NM/\epsilon)$.

C. Reference state preparation

One may use any reference state at each step of the recursive coherent state addition, provided that ζ_3 and ζ_4 are both positive. Regardless of the choice of reference states, superposition states to be computed are identical within a tolerant error. However, the choice of reference states affects the computational complexity; the larger ζ_3 and ζ_4 are, the shorter the computational time is.

A set of reference states with large ζ_3 and ζ_4 may be found by a variational quantum algorithm. Let $U_k(\boldsymbol{\theta}_k)$ be an ansatz quantum circuit for generating a reference state of step k : $U_k(\boldsymbol{\theta}_k) |0\rangle = |\chi_{\text{add}}^k(\boldsymbol{\theta}_k)\rangle$. Here, $\boldsymbol{\theta}_k$ denotes circuit parameters to be optimized. In this setup, ζ_3 and ζ_4 are considered as functions of $\{\boldsymbol{\theta}_k\}$. The optimal values of $\{\boldsymbol{\theta}_k\}$ can be found by solving the following optimization problem:

$$\text{maximize}_{\{\boldsymbol{\theta}_k\}} \min\{\zeta_3(\{\boldsymbol{\theta}_k\}), \zeta_4(\{\boldsymbol{\theta}_k\})\}. \quad (\text{S99})$$

Using a solution of the optimization problem, denoted by $\{\boldsymbol{\theta}_k^*\}$, the reference state of each step k is prepared by $U_k(\boldsymbol{\theta}_k^*)$.

We can also compute a set of reference states such that $1/\zeta_3 = O(1)$ and $1/\zeta_4 = O(1)$ with another protocol. These conditions on ζ_3 and ζ_4 imply that the required number of quantum SVDs for computing a DMD mode state is $O(\text{poly } R)$. In what follows, we present a specific procedure for reference state preparation satisfying these conditions.

Initially, we perform pure-state tomography [3] to estimate all right singular vector states of $[\mathbf{X} \ \mathbf{X}']$. The pure-state tomography requires an $O(M)$ runtime for each right singular vector state. Subsequently, for each right singular vector state $|\mathbf{v}_{r'}^{[\mathbf{X} \ \mathbf{X}']*}\rangle$, we construct a quantum circuit $V_{r'}$ such that $V_{r'}|0\rangle = \exp(-i\varphi_{r'})|\mathbf{v}_{r'}^{[\mathbf{X} \ \mathbf{X}']*}\rangle$. Here $\varphi_{r'}$ signifies an unknown global phase which cannot be determined by the pure-state tomography. When the classical data of the amplitudes of $|\mathbf{v}_{r'}^{[\mathbf{X} \ \mathbf{X}']*}\rangle$ is given, such a quantum circuit can be implemented with a gate complexity of $O(\text{poly log } M)$ [4, 5].

Next, we show that a superposition state of the form

$$\sum_{r'=1}^R \alpha_{r'} e^{i\varphi_{r'}} |\mathbf{u}_{r'}^{[\mathbf{X} \ \mathbf{X}']}\rangle \quad (\text{S100})$$

can be computed for arbitrary user-specified amplitudes $\boldsymbol{\alpha} = [\alpha_1, \dots, \alpha_R]^\top$ such that $\|\boldsymbol{\alpha}\| = 1$, using the quantum SVD and controlled- $V_{r'}^\dagger$ operations. The computation is composed of the following steps: (1) Prepare $|\text{SVD}([\mathbf{X} \ \hat{\mathbf{X}}'])\rangle_{1,5}$. (2) Uncompute the second to fourth registers by controlled- $V_{r'}^\dagger$ operations conditioned on the fifth register:

$$\begin{aligned} & \sum_{r'=1}^R \hat{\sigma}_{r'}^{[\mathbf{X} \ \mathbf{X}']} |\mathbf{u}_{r'}^{[\mathbf{X} \ \mathbf{X}']}\rangle_1 V_{r'}^\dagger |\mathbf{v}_{r'}^{[\mathbf{X} \ \mathbf{X}']*}\rangle_{234} |(\hat{\sigma}_{r'}^{[\mathbf{X} \ \mathbf{X}']})^2\rangle_5 \\ &= \sum_{r'=1}^R \hat{\sigma}_{r'}^{[\mathbf{X} \ \mathbf{X}']} e^{i\varphi_{r'}} |\mathbf{u}_{r'}^{[\mathbf{X} \ \mathbf{X}']}\rangle_1 |0\rangle_{234} |(\hat{\sigma}_{r'}^{[\mathbf{X} \ \mathbf{X}']})^2\rangle_5. \end{aligned} \quad (\text{S101})$$

(3) Append an ancilla qubit as the sixth register. (4) Apply controlled rotations of the ancilla qubit conditioned on the fifth register to yield

$$\sum_{r'=1}^R \hat{\sigma}_{r'}^{[\mathbf{X} \ \mathbf{X}']} e^{i\varphi_{r'}} |\mathbf{u}_{r'}^{[\mathbf{X} \ \mathbf{X}']}\rangle_1 |0\rangle_{234} |(\hat{\sigma}_{r'}^{[\mathbf{X} \ \mathbf{X}']})^2\rangle_5 \left[\frac{a\alpha_{r'}}{\hat{\sigma}_{r'}^{[\mathbf{X} \ \mathbf{X}']}} |0\rangle_6 + \sqrt{1 - \left| \frac{a\alpha_{r'}}{\hat{\sigma}_{r'}^{[\mathbf{X} \ \mathbf{X}']}} \right|^2} |1\rangle_6 \right], \quad (\text{S102})$$

where

$$a = \min_{r'} \left| \frac{\hat{\sigma}_{r'}^{[\mathbf{X} \ \mathbf{X}']}}{\alpha_{r'}} \right|. \quad (\text{S103})$$

(5) Uncompute the fifth register by the inverse operation of the quantum SVD. (6) Measure the second to sixth registers. If all measured values are zero, we obtain the target superposition state. The success probability is $|a|^2$, bounded from below as

$$|a|^2 \geq \min_{r'} (\hat{\sigma}_{r'}^{[\mathbf{X} \ \mathbf{X}']})^2 = \Omega \left(\frac{1}{\kappa_{[\mathbf{X} \ \mathbf{X}']}^2 R} \right). \quad (\text{S104})$$

Here, $\kappa_{[\mathbf{X} \ \mathbf{X}']}^2$ is the condition number of $[\mathbf{X} \ \mathbf{X}']$ (see Eq. (S8)), and we use Eq. (S16) to derive the lower bound. Therefore, the required number of quantum SVDs for this computation is $O(\kappa_{[\mathbf{X} \ \mathbf{X}']}^2 R)$.

It is worth noting that the target superposition state created by the above protocol contains unknown phase factors $\exp(i\varphi_{r'})$; thus the above protocol cannot be utilized for computing DMD mode states. However, this protocol has less computational complexity compared with the recursive coherent state addition protocol and is helpful for preparing reference states as described below. Hereinafter, we call the above protocol as *out-of-phase superposition protocol*.

The reference state $|\chi_{\text{add}}^k\rangle$ of step k that we aim to compute using the out-of-phase superposition protocol is given by

$$|\chi_{\text{add}}^k\rangle = \frac{1}{\sqrt{2}} \left[e^{i\varphi_0^k} |\psi_{I_0^k}\rangle + e^{i\varphi_1^k} |\psi_{I_1^k}\rangle \right], \quad (\text{S105})$$

where φ_j^k 's signify arbitrary relative phases. This reference state of step k is computable for any k , which is proven by the following mathematical induction with respect to the recursion depth. (1) For any step k that corresponds to one of the deepest branch nodes of the recursion tree (see Fig. S1), $|\psi_{I_j^k}\rangle$'s are left singular vector states of $[\mathbf{X} \ \mathbf{X}']$, thus $|\chi_{\text{add}}^k\rangle$ defined above is computable by the out-of-phase superposition protocol. (2) For step k that does not

correspond to one of the deepest branch nodes, assume that the reference states for all descendant nodes of step k are computable. Let k_c denote the index of a child node of step k . Due to the induction hypothesis, we can compute $|\psi_{I_0^{k_c} \cup I_1^{k_c}}\rangle$ by recursively performing the two-state coherent addition steps of the descendant nodes with the reference states defined in Eq. (S105). Furthermore, we can compute the following state with control parameter $\vartheta^{k_c} \in [0, 2\pi)$ using the out-of-phase superposition protocol:

$$\begin{aligned} |\tilde{\psi}_{I_0^{k_c} \cup I_1^{k_c}}(\vartheta^{k_c})\rangle &= \frac{e^{i\varphi_0^{k_c}}}{\sqrt{\sum_{r' \in I_0^{k_c} \cup I_1^{k_c}} |\tilde{w}_{r'}^{r'}|^2}} \sum_{r' \in I_0^{k_c}} \tilde{w}_{r'}^{r'} |\mathbf{u}_{r'}^{[\mathbf{X} \ \mathbf{X}']}\rangle \\ &+ \frac{e^{i(\varphi_1^{k_c} + \vartheta^{k_c})}}{\sqrt{\sum_{r' \in I_0^{k_c} \cup I_1^{k_c}} |\tilde{w}_{r'}^{r'}|^2}} \sum_{r' \in I_1^{k_c}} \tilde{w}_{r'}^{r'} |\mathbf{u}_{r'}^{[\mathbf{X} \ \mathbf{X}']}\rangle. \end{aligned} \quad (\text{S106})$$

The user-specified amplitudes for computing this state by the out-of-phase superposition protocol is given by

$$\boldsymbol{\alpha}^{k_c}(\vartheta^{k_c}) = \sqrt{\frac{2 \sum_{r' \in I_0^{k_c}} |\tilde{w}_{r'}^{r'}|^2}{\sum_{r' \in I_0^{k_c} \cup I_1^{k_c}} |\tilde{w}_{r'}^{r'}|^2}} \boldsymbol{\alpha}_0^{k_c} + e^{i\vartheta^{k_c}} \sqrt{\frac{2 \sum_{r' \in I_1^{k_c}} |\tilde{w}_{r'}^{r'}|^2}{\sum_{r' \in I_0^{k_c} \cup I_1^{k_c}} |\tilde{w}_{r'}^{r'}|^2}} \boldsymbol{\alpha}_1^{k_c}. \quad (\text{S107})$$

Here, $\boldsymbol{\alpha}_j^{k_c}$ is a vector whose r' -th element is the user-specified amplitude of $|\mathbf{u}_{r'}^{[\mathbf{X} \ \mathbf{X}']}\rangle$ used to compute $|\chi_{\text{add}}^{k_c}\rangle$ if $r' \in I_j^{k_c}$ or zero otherwise. Note that $\boldsymbol{\alpha}_j^{k_c}$'s are known due to the induction hypothesis. This state $|\tilde{\psi}_{I_0^{k_c} \cup I_1^{k_c}}(\vartheta^{k_c})\rangle$ is similar to the state $|\psi_{I_0^{k_c} \cup I_1^{k_c}}\rangle$. The fidelity of these two states, i.e., $|\langle \tilde{\psi}_{I_0^{k_c} \cup I_1^{k_c}}(\vartheta^{k_c}) | \psi_{I_0^{k_c} \cup I_1^{k_c}} \rangle|^2$, takes a maximum value of one if and only if $\vartheta^{k_c} = \varphi_0^{k_c} - \varphi_1^{k_c}$. The maximizer ϑ^{k_c*} of the fidelity can be found through a grid search based on the fidelity measurement. The quantum state $|\tilde{\psi}_{I_0^{k_c} \cup I_1^{k_c}}(\vartheta^{k_c*})\rangle$ is equivalent to $|\psi_{I_0^{k_c} \cup I_1^{k_c}}\rangle$ ($= |\psi_{I_j^k}\rangle$) up to a global phase. In this way, we can compute the user-specified amplitudes $\boldsymbol{\alpha}^{k_c}(\vartheta^{k_c*})$ to compute $|\psi_{I_j^k}\rangle$ by the out-of-phase superposition protocol. By employing $\sum_{k_c} \boldsymbol{\alpha}^{k_c}(\vartheta^{k_c*})/\sqrt{2}$ as a user-specified amplitude vector, we are able to compute the reference state of the form given in Eq. (S105) using the out-of-phase superposition protocol. This concludes the proof.

The above proof shows that we can recursively determine an appropriate amplitude vector to compute $|\psi_{I_j^k}\rangle$ using the out-of-phase superposition protocol. Therefore, $|\psi_{I_0^k \cup I_1^k}\rangle$ is computable by a *single-step* coherent addition of the two states $|\psi_{I_0^k}\rangle$ and $|\psi_{I_1^k}\rangle$, which are prepared with the out-of-phase superposition protocol. This quantum process has an advantage in the success probability compared with the *multistep* recursive coherent addition, because the success probability of the recursive coherent addition decreases exponentially with respect to the recursion depth. In addition, the presented quantum process for computing $|\chi_{\text{add}}^k\rangle$ is not unitary but a block encoding of the unitary gate $U_{\chi_{\text{add}}^k}$. Even in this case, it is still possible to perform the coherent addition, although the success probability decreases by a factor of $\Omega(1/\kappa_{[\mathbf{X} \ \mathbf{X}']}^2 R)$. Given these facts, the necessary number of quantum SVDs to compute $|\psi_{I_0^k \cup I_1^k}\rangle$ by the single-step coherent addition is estimated as $O(\kappa_{[\mathbf{X} \ \mathbf{X}']}^4 R^2/\zeta_4)$.

The reference states defined in Eq. (S105) satisfy

$$|\langle \chi_{\text{add}}^k | \psi_{I_j^k} \rangle|^2 = \frac{1}{2} \quad (\text{S108})$$

for all k and j ; thus $1/\zeta_4 = 2$. In contrast, $|\langle \chi_1 | \chi_{\text{add}}^k \rangle|$ could be close to zero for some k , leading to a situation where $1/\zeta_3$ becomes excessively large. This problem can be resolved by the following modification: Let b be a positive constant less than $1/\sqrt{2}$. When the reference state satisfies $|\langle \chi_1 | \chi_{\text{add}}^k \rangle| \leq b/2$, we modify the reference state to $|\chi_{\text{add}'}^k\rangle$:

$$|\chi_{\text{add}'}^k\rangle = \mathcal{C}_{\text{add}'}^k [|\chi_{\text{add}}^k\rangle + b|\chi_1\rangle], \quad (\text{S109})$$

where $\mathcal{C}_{\text{add}'}^k$ denotes the normalizing constant. The normalizing constant is bounded from below as

$$\begin{aligned} \mathcal{C}_{\text{add}'}^k &= \frac{1}{\| |\chi_{\text{add}}^k\rangle + b|\chi_1\rangle \|} \\ &\geq \frac{1}{\| |\chi_{\text{add}}^k\rangle \| + b\| |\chi_1\rangle \|} = \frac{1}{1+b}. \end{aligned} \quad (\text{S110})$$

Therefore, the modified reference state satisfies

$$\begin{aligned} |\langle \chi_1 | \chi_{\text{add}'}^k \rangle| &\geq \mathcal{C}_{\text{add}'}^k [b |\langle \chi_1 | \chi_1 \rangle| - |\langle \chi_1 | \chi_{\text{add}}^k \rangle|] \\ &\geq \frac{1}{1+b} \left(b - \frac{b}{2} \right) = \frac{b}{2(1+b)}, \end{aligned} \quad (\text{S111})$$

and

$$\begin{aligned} |\langle \chi_{\text{add}'}^k | \psi_{I_j^k} \rangle| &\geq \mathcal{C}_{\text{add}'}^k \left[|\langle \chi_{\text{add}}^k | \psi_{I_j^k} \rangle| - b |\langle \chi_1 | \psi_{I_j^k} \rangle| \right] \\ &\geq \frac{1}{1+b} \left(\frac{1}{\sqrt{2}} - b \right) > 0. \end{aligned} \quad (\text{S112})$$

Consequently, $1/\zeta_3 = O(1)$ and $1/\zeta_4 = O(1)$.

In summary, the overall number of quantum SVDs necessary for computing a DMD mode state through the presented protocol scales as $\tilde{O}(R^2)$ with respect to R , although the protocol requires the pure state tomography with $O(MR)$ complexity. Here, \tilde{O} indicates that polylogarithmic factors are omitted. The gate complexity is larger than the required number of quantum SVDs by a factor of $T/\epsilon^2 \text{poly} \log(NM/\epsilon)$.

IV. COMPARISON OF THE qDMD AND RELATED ALGORITHMS

This section compares the qDMD algorithm proposed in the present study with the related algorithms presented in previous studies [9–14].

A. Time Series Analysis Algorithms

First, we compare the qDMD algorithm with two quantum algorithms for time series analysis, namely, (1) quantum matrix pencil method (QMPM) proposed by Steffens et al. [9] and (2) a quantum dynamic mode decomposition (QDMD⁴) algorithm proposed by Xue et al. [10]. Table SII provides a summary of this comparison.

All the time series analysis algorithms aim to decompose time series data into modes with exponential decay/growth and/or sinusoidal oscillation. The qDMD and QDMD algorithms analyze N -dimensional time series data with length M , while the QMPM algorithm analyzes one-dimensional data with length T . All the algorithms are based on similar quantum-classical hybrid strategies which consist of (i) estimating a matrix such as $\tilde{\mathbf{K}}'$ using a quantum computer, (ii) solving the eigenvalue problem of the estimated matrix on a classical computer, and (iii) computing mode states on a quantum computer. Since the QMPM algorithm analyzes one-dimensional data, it does not include the mode state computing step.

The main difference between these algorithms lies in their input data. The input to the qDMD algorithm is quantum states computed by a quantum differential equation solver. On the other hand, the QMPM and QDMD

TABLE SII. Comparison of three quantum algorithms for time series analysis.

Algorithm	Time Series Data Input Method	Matrix Estimation Complexity	Mode State Computation Complexity
qDMD (present study)	Quantum states computed by a quantum differential equation solver	$\tilde{O} \left(\frac{\kappa^2 R^2 T}{\zeta^2 \epsilon^4} \text{poly} \log NM \right)$	$\tilde{O} \left(\frac{\kappa^2 R^{2+\log_2(1/\zeta_4)} T}{\epsilon^2} \text{poly} \log NM \right)$
QMPM [9]	Quantum oracles that have random access to time series data	$\tilde{O} \left(\frac{\xi_{\text{QMPM}} R^2}{\epsilon^4} \text{poly} \log T \right)$	N/A
QDMD [10]	Quantum oracles that have random access to time series data	$\tilde{O} \left(\frac{\kappa^5 R^6 M^{3.5}}{\epsilon^3} \text{poly} \log NM \right)$	$\tilde{O} (\kappa M \text{poly} \log NM)$

⁴ Xue et al. named their algorithm “QDMD,” while we call our algorithm “qDMD” because the DMD community sometimes prefixes the name of variants with lowercase letters. To avoid confusion, we also refer to the QDMD algorithm as “QRAM-based QDMD” in the text because the algorithm requires quantum random access memory (QRAM).

algorithms require quantum oracles⁵ that have random access to, for example, a time series data element x_j^i . The implementation of such quantum random access memories (QRAMs) presents technical challenges, as also highlighted in [15]. A QRAM may need to access a classical data structure that stores the time series data [4]. Given that the time series data comprises NM entries in this study, constructing such a QRAM may require computation time and memory of the order of $O(NM)$. Therefore, these QRAM-based algorithms are likely not suitable for analyzing high-dimensional differential equations when N is too large for classical computers to handle. Additionally, the QMPM algorithm is inherently designed for one-dimensional time series data and does not address the high-dimensional cases considered here.

The computational complexity of matrix estimation (i) and that of mode state computation (iii) for each algorithm are listed in Table SII. In the table, we omit polylogarithmic factors in the computational complexities by use of the symbol \tilde{O} , except for the data size parameters N , M , and T . The parameter κ denotes the maximum condition number among matrices \mathbf{X} , \mathbf{X}' , and $[\mathbf{X} \ \mathbf{X}']$ (see Eq. (S8)). The parameters ζ and ζ_4 are defined in Eqs. (S10) and (S95), respectively. The parameter ξ_{QMPM} is related to sampling efficiency in the QMPM algorithm [9].

All algorithms achieve exponential speedups in the dimensionality N and/or the time series data length T or M . However, the computational complexities of the QRAM-based algorithms listed in the table *do not* include the cost of time series data computation, while the computational complexity of the qDMD algorithm *does* include it. As noted above, when the time series computation cost is taken into account, the computational complexities of the QRAM-based algorithms may be exponentially larger than those listed in the table with respect to T (for QMPM) or N (for QDMD). In regard to other parameters, the QRAM-based QDMD algorithm is better than the others in terms of ϵ , but our qDMD algorithm outperforms the QRAM-based QDMD algorithm in terms of M .

B. Quantum Eigensolvers for Complex Eigenvalue Problems

Second, we compare the qDMD algorithm with four quantum eigensolvers for complex eigenvalue problems, namely, (1) measurement-based phase estimation algorithm (MPEA) proposed by Wang et al. [11], (2) iterative phase estimation algorithm with universal circuit for non-unitary matrices (IPEA+UCNUM) proposed by Daskin et al. [12],

TABLE SIII. Comparison of quantum eigensolvers for complex eigenvalue problems. In the table, \mathbf{A} denotes the $N \times N$ target matrix of an eigenvalue problem, and \hat{A} signifies the operator form of \mathbf{A} .

Algorithm	Requirements	Outputs	Exponential Speedup in N
qDMD (present study)	(1) $\dot{\mathbf{x}} = \mathbf{A}\mathbf{x}$ can be simulated efficiently on a quantum computer and (2) the number of dominant eigenstates in the initial state is $O(\text{poly log } N)$.	Eigenvalues and eigenstates	YES
MPEA [11]	There exist a pure state $ \phi\rangle$ of an ancillary system, a Hamiltonian operator \hat{H} acting on the target and ancillary systems, and a positive constant Δt such that $\hat{A} = \langle \phi \exp(-i\hat{H}\Delta t) \phi \rangle$.	The eigenvalue with the largest absolute value and its eigenstate	YES
IPEA+UCNUM [12]	An eigenstate can be prepared.	The eigenvalue of the prepared state	NO
QAE [13]	\mathbf{A} is Hermitian or symmetric.	Eigenvalues and eigenvectors (classical data)	NO
PEA+QLDES [14]	(1) $\dot{\mathbf{y}} = i\pi(\mathbf{A} \otimes \mathbf{I} + \mathbf{I} \otimes \mathbf{A}^*)\mathbf{y}$ can be simulated efficiently and (2) an initial state $\mathbf{y}_0 = \sum_i c_i(\mathbf{v}_i \otimes \mathbf{v}_i^*)$ can be prepared efficiently on a quantum computer (\mathbf{v}_i : the i -th eigenvector, c_i : a complex constant, $*$: complex conjugate).	Eigenvalues and eigenstates	YES

⁵ Steffens et al. also proposed another version of the QMPM algorithm where the input is quantum states encoding time series data in a particular form. However, how to prepare such particular quantum states remains an open question, and the main focus of the study is on the oracular setting [9].

(3) quantum annealer eigensolver (QAE) proposed by Teplukhin et al. [13], and (4) phase estimation algorithm with a quantum linear differential equation solver (PEA+QLDES) proposed by Shao [14]. Table SIII provides a summary of this comparison.

The first algorithm, MPEA, is a quantum analog of the power method for solving eigenvalue problems. The algorithm iteratively applies a non-unitary operator \hat{A} to a state vector of the target system. The operator \hat{A} is realized through Hamiltonian simulation and a projective measurement as $\hat{A} = \langle \phi | \exp(-i\hat{H}\Delta t) | \phi \rangle$. Here, $|\phi\rangle$ is a pure state of an ancillary system, \hat{H} denotes the Hamiltonian governing the dynamics of the target and ancillary systems, and Δt signifies the time step parameter. After applying \hat{A} to an initial state $|\psi_0\rangle$ a sufficient number of times, one can obtain the eigenstate of \hat{A} with the maximum eigenvalue (in absolute value) among all eigenstates included in $|\psi_0\rangle$. The MPEA is expected to achieve an exponential speedup in the dimensionality of the target system N . However, the success probability of the power iteration may decrease exponentially as the number of iterations increases, leading to a decrease in the algorithm's efficiency.

The second method applies the iterative phase estimation to the non-unitary time evolution realized through a universal circuit design for arbitrary non-unitary operations. This algorithm estimates the complex eigenvalue associated with a prepared eigenstate. Because the complexity of the non-unitary operation is $O(N^2)$, this algorithm does not guarantee an exponential speedup in N .

The third algorithm, QAE, is a variational algorithm on quantum annealing devices. This method can estimate complex eigenvalues and their eigenvectors of complex Hermitian or symmetric matrices. Note that this algorithm outputs eigenvectors as classical data instead of quantum states. This method also does not guarantee an exponential speedup in N .

The fourth algorithm applies the phase estimation method to time series data simulated by a QLDES. The algorithm simulates the linear differential equation, defined as $\dot{\mathbf{y}} = i\pi(\mathbf{A} \otimes \mathbf{I} + \mathbf{I} \otimes \mathbf{A}^*)\mathbf{y}$. Here, \mathbf{A}^* designates the complex conjugate of \mathbf{A} . The initial state of the simulation must be $\mathbf{y}_0 = \sum_i c_i (\mathbf{v}_i \otimes \mathbf{v}_i^*)$, where \mathbf{v}_i and \mathbf{v}_i^* denote the i -th eigenvector and its complex conjugate, respectively, and c_i is an arbitrary complex constant. This algorithm can compute complex eigenvalues and their eigenstates in time $O(\text{poly log } N)$. However, it remains an open problem how to prepare the initial state of the particular form without knowledge of the eigenstates. Therefore, the author concluded that this algorithm is impractical for complex eigenvalue problems [14].

The proposed qDMD algorithm requires that (1) $\dot{\mathbf{x}} = \mathbf{A}\mathbf{x}$ can be simulated efficiently on a quantum computer and (2) the number of dominant eigenstates in the initial state, i.e., R , is $O(\text{poly log } N)$. These requirements are analogous to those in quantum phase estimation algorithm for the eigenvalue problem of a Hermitian matrix \mathbf{H} [16]: (1) $\dot{\mathbf{x}} = -i\mathbf{H}\mathbf{x}$ can be simulated efficiently on a quantum computer and (2) the initial state includes $O(\text{poly log } N)$ dominant eigenstates of which eigenvalues are to be estimated. Under these requirements, the qDMD algorithm provides an exponential speedup with respect to N for finding complex eigenvalues and eigenvectors.

V. DYNAMIC MODE DECOMPOSITION FOR DEFECTIVE SYSTEMS

The qDMD algorithm presented in the main text assumes that the matrix \mathbf{A} is diagonalizable. This assumption implies that \mathbf{K} is also diagonalizable, thus its projected approximation $\tilde{\mathbf{K}}'$ is assumed to have the eigenvalue decomposition. In this section, we consider a situation where \mathbf{A} is not diagonalizable. Such a non-diagonalizable matrix is said to be *defective* [17].

Any square matrix $\mathbf{A} \in \mathbb{C}^{N \times N}$ can be expressed in the Jordan normal form [17] as

$$\mathbf{A} = \mathbf{P} \begin{pmatrix} \mathbf{J}_1 & & \\ & \ddots & \\ & & \mathbf{J}_p \end{pmatrix} \mathbf{P}^{-1}, \quad (\text{S113})$$

where \mathbf{P} is an $N \times N$ invertible matrix, \mathbf{J}_k ($k = 1, \dots, p$) denotes a Jordan block. The k -th Jordan block is defined by

$$\mathbf{J}_k = \begin{pmatrix} \lambda_k^{\mathbf{A}} & 1 & & \\ & \lambda_k^{\mathbf{A}} & \ddots & \\ & & \ddots & 1 \\ & & & \lambda_k^{\mathbf{A}} \end{pmatrix} \in \mathbb{C}^{m_k \times m_k}, \quad (\text{S114})$$

where $\lambda_k^{\mathbf{A}}$ is an eigenvalue of \mathbf{A} , and m_k is the order of the Jordan block. The block diagonal matrix $\text{diag}(\mathbf{J}_1, \dots, \mathbf{J}_p)$ is called as the Jordan normal form of \mathbf{A} . If $m_k = 1$ for all $k \in \{1, \dots, p\}$, the Jordan normal form is a diagonal

matrix, thus \mathbf{A} is diagonalizable; otherwise, \mathbf{A} is defective. Using the Jordan normal form, we can calculate the time-evolution operator \mathbf{K} as

$$\begin{aligned} \mathbf{K} &= \exp(\Delta t \mathbf{A}) \\ &= \mathbf{P} \begin{pmatrix} \exp(\Delta t \mathbf{J}_1) & & \\ & \ddots & \\ & & \exp(\Delta t \mathbf{J}_p) \end{pmatrix} \mathbf{P}^{-1}. \end{aligned} \quad (\text{S115})$$

The exponential of a Jordan block is given by

$$\exp(\Delta t \mathbf{J}_k) = e^{\Delta t \lambda_k^{\mathbf{A}}} \begin{pmatrix} 1 & \frac{\Delta t}{1!} & \cdots & \frac{(\Delta t)^{m_k-1}}{(m_k-1)!} \\ & 1 & \ddots & \vdots \\ & & \ddots & \frac{\Delta t}{1!} \\ & & & 1 \end{pmatrix} \in \mathbb{C}^{m_k \times m_k}. \quad (\text{S116})$$

For $\Delta t \neq 0$, this exponential $\exp(\Delta t \mathbf{J}_k)$ has only one eigenvalue $\exp(\Delta t \lambda_k^{\mathbf{A}})$ with geometric multiplicity one. Therefore, the Jordan normal form of \mathbf{K} is the same as that of \mathbf{A} except that each eigenvalue $\lambda_k^{\mathbf{A}}$ is replaced by $\exp(\Delta t \lambda_k^{\mathbf{A}})$.

The qDMD algorithm, as well as the classical exact DMD algorithm [18], can estimate the time-evolution operator \mathbf{K} through $\tilde{\mathbf{K}}'$ even for a defective system. This is because $\tilde{\mathbf{K}}'$ is defined through the singular value decompositions of data matrices, where no assumption is made on the diagonalizability. However, for a defective system, $\tilde{\mathbf{K}}'$ is (nearly) defective⁶, thus the eigenvalue decomposition of $\tilde{\mathbf{K}}'$ is infeasible. The Schur-based DMD algorithm proposed by Thitsa et al. [19] is a numerically-stable DMD algorithm for such a (nearly) defective system. The Schur-based DMD algorithm computes the Schur decomposition of $\tilde{\mathbf{K}}'$, instead of its eigenvalue decomposition. The Schur decomposition of $\tilde{\mathbf{K}}'$ is given by

$$\tilde{\mathbf{K}}' = \tilde{\mathbf{W}}'_{\text{Schur}} \tilde{\mathbf{S}}' \tilde{\mathbf{W}}'^{\dagger}_{\text{Schur}}, \quad (\text{S117})$$

where $\tilde{\mathbf{S}}'$ is an upper triangular matrix, and $\tilde{\mathbf{W}}'_{\text{Schur}}$ is a unitary matrix. This decomposition provides an approximation of the Schur decomposition of $\tilde{\mathbf{K}}$,

$$\tilde{\mathbf{K}} = \tilde{\mathbf{W}}_{\text{Schur}} \tilde{\mathbf{S}} \tilde{\mathbf{W}}^{\dagger}_{\text{Schur}}, \quad (\text{S118})$$

as

$$\tilde{\mathbf{S}} \approx \tilde{\mathbf{S}}', \quad (\text{S119})$$

$$\tilde{\mathbf{W}}_{\text{Schur}} \approx \mathbf{Q} \tilde{\mathbf{W}}'_{\text{Schur}}. \quad (\text{S120})$$

Here, \mathbf{Q} is an $N \times R$ matrix whose columns are the R dominant left singular vectors of $[\mathbf{X} \ \mathbf{X}']$. The column vectors of the transformation matrix $\tilde{\mathbf{W}}_{\text{Schur}}$ can be computed in the same manner as step 5 of the qDMD algorithm presented in the main text. Therefore, the quantum procedures (steps 1–3 and 5) of the qDMD algorithm can be directly adapted to the quantum version of the Schur-based DMD algorithm for nearly defective systems.

-
- [1] R. K. Brayton, On the asymptotic behavior of the number of trials necessary to complete a set with random selection, *Journal of Mathematical Analysis and Applications* **7**, 31 (1963).
 - [2] S. Kimmel, C. Y.-Y. Lin, G. H. Low, M. Ozols, and T. J. Yoder, Hamiltonian simulation with optimal sample complexity, *npj Quantum Information* **3**, 13 (2017).
 - [3] F. Verdeil and Y. Deville, Pure-state tomography with parallel unentangled measurements, *Physical Review A* **107**, 012408 (2023).
 - [4] I. Kerenidis and A. Prakash, Quantum recommendation systems, in *8th Innovations in Theoretical Computer Science Conference (ITCS 2017)*, Leibniz International Proceedings in Informatics (LIPIcs), Vol. 67 (Schloss Dagstuhl–Leibniz-Zentrum fuer Informatik, 2017) p. 49.

⁶ The Jordan normal form of \mathbf{K} may be structurally unstable; small perturbations due to finite computational precision and estimation errors may make $\tilde{\mathbf{K}}$ not strictly defective. In general, it is impossible to determine whether a matrix is defective or not in the presence of computational errors [17].

- [5] K. Mitarai, M. Kitagawa, and K. Fujii, Quantum analog-digital conversion, *Physical Review A* **99**, 012301 (2019).
- [6] M. Schuld, I. Sinayskiy, and F. Petruccione, Prediction by linear regression on a quantum computer, *Physical Review A* **94**, 022342 (2016).
- [7] T. Shirakawa, H. Ueda, and S. Yunoki, Automatic quantum circuit encoding of a given arbitrary quantum state (2021), arXiv:2112.14524 [quant-ph].
- [8] M. Oszmaniec, A. Grudka, M. Horodecki, and A. Wójcik, Creating a superposition of unknown quantum states, *Physical Review Letters* **116**, 110403 (2016).
- [9] A. Steffens, P. Rebentrost, I. Marvian, J. Eisert, and S. Lloyd, An efficient quantum algorithm for spectral estimation, *New Journal of Physics* **19**, 033005 (2017).
- [10] C. Xue, Z.-Y. Chen, T.-P. Sun, X.-F. Xu, S.-M. Chen, H.-Y. Liu, X.-N. Zhuang, Y.-C. Wu, and G.-P. Guo, Quantum dynamic mode decomposition algorithm for high-dimensional time series analysis, *Intelligent Computing* **2**, 0045 (2023).
- [11] H. Wang, L.-A. Wu, Y.-x. Liu, and F. Nori, Measurement-based quantum phase estimation algorithm for finding eigenvalues of non-unitary matrices, *Physical Review A* **82**, 062303 (2010).
- [12] A. Daskin, A. Grama, and S. Kais, A universal quantum circuit scheme for finding complex eigenvalues, *Quantum Information Processing* **13**, 333 (2014).
- [13] A. Teplukhin, B. K. Kendrick, and D. Babikov, Solving complex eigenvalue problems on a quantum annealer with applications to quantum scattering resonances, *Physical Chemistry Chemical Physics* **22**, 26136 (2020).
- [14] C. Shao, Computing eigenvalues of diagonalizable matrices on a quantum computer, *ACM Transactions on Quantum Computing* **3**, 1 (2022).
- [15] B. T. Kiani, G. De Palma, D. Englund, W. Kaminsky, M. Marvian, and S. Lloyd, Quantum advantage for differential equation analysis, *Physical Review A* **105**, 022415 (2022).
- [16] D. S. Abrams and S. Lloyd, Quantum algorithm providing exponential speed increase for finding eigenvalues and eigenvectors, *Physical Review Letters* **83**, 5162 (1999).
- [17] G. H. Golub and J. H. Wilkinson, Ill-conditioned eigensystems and the computation of the Jordan canonical form, *SIAM review* **18**, 578 (1976).
- [18] J. H. Tu, C. W. Rowley, D. Luchtenburg, S. L. Brunton, and J. N. Kutz, On dynamic mode decomposition: Theory and applications, *Journal of Computational Dynamics* **1**, 391 (2014).
- [19] M. Thitsa, M. Cloutre, E. Verriest, S. Coogan, and C. Martin, A numerically stable dynamic mode decomposition algorithm for nearly defective systems, *IEEE Control Systems Letters* **5**, 67 (2020).